

February 2008

Non-Gaussianity, Spectral Index and Tensor Modes in Mixed Inflaton and Curvaton Models

Kazuhide Ichikawa¹, Teruaki Suyama¹, Tomo Takahashi²
and Masahide Yamaguchi³

¹ *Institute for Cosmic Ray Research, University of Tokyo, Kashiwa 277-8582, Japan*

² *Department of Physics, Saga University, Saga 840-8502, Japan*

³ *Department of Physics and Mathematics,
Aoyama Gakuin University, Sagami-hara 229-8558, Japan*

Abstract

We study non-Gaussianity, the spectral index of primordial scalar fluctuations and tensor modes in models where fluctuations from the inflaton and the curvaton can both contribute to the present cosmic density fluctuations. Even though simple single-field inflation models generate only tiny non-Gaussianity, if we consider such a mixed scenario, large non-Gaussianity can be produced. Furthermore, we study the inflationary parameters such as the spectral index and the tensor-to-scalar ratio in this kind of models and discuss in what cases models predict the spectral index and tensor modes allowed by the current data while generating large non-Gaussianity, which may have many implications for model-buildings of the inflationary universe.

1 Introduction

It is widely believed that cosmic microwave background anisotropies and large scale structure of the universe we observe today originate from fluctuations generated during the time of inflation. It is often assumed that the quantum fluctuation of the inflaton is responsible for that. During inflation, the inflaton slowly rolls down its potential, which gives almost scale-invariant primordial fluctuations and some gravity waves can also be generated. Usually the primordial fluctuations are characterized by the scalar spectral index and the tensor-to-scalar ratio. Once the potential for the inflaton is given, one can predict these quantities to compare with cosmological observations. Current cosmological data are very precise to severely constrain models of inflation and some models are considered to have been already excluded [1, 2].

In fact, the considerations of the spectral index and tensor modes may not be enough to probe primordial fluctuations. The non-Gaussianity of the fluctuations can also be measured by cosmological observations and be used to test the scenario generating primordial fluctuations. In particular, there has recently been reported that non-Gaussianity is detected in the cosmic microwave background almost at 3σ level [3]. Since simple single-field inflation models predict very small non-Gaussianity, if the evidence for large non-Gaussianity is mounting in the future, these models which at present are judged to be successful as regards the amplitude and scale dependence for primordial curvature fluctuations may suffer from a great difficulty.

However, notice that another source of fluctuations other than the inflaton can contribute to the cosmic density fluctuations. Among such possibilities, the curvaton mechanism [4, 5, 6] and modulated reheating scenarios [7, 8], for example, have been proposed and some of their observational consequences including issues of the non-Gaussianity have also been investigated. In particular, it is discussed that large non-Gaussianity can be produced in these scenarios. It should be reminded that cosmic density fluctuations can originate from one of these mechanisms including the inflaton or from some combination of these. Thus, even though almost perfect Gaussian fluctuations are generated in simple inflation models where they originate only from the inflaton, large non-Gaussianity can be produced for total by adding the contribution from another generation mechanism. One of the purposes of this paper is to study the issue of non-Gaussianity in models of this kind, paying particular attention to a mixed scenario where fluctuations of the inflaton and the curvaton can both contribute to primordial fluctuations. In investigating the non-Gaussianity, we focus not only on the bispectrum but also on the trispectrum which is a potentially useful observable in the near future.

It should also be noticed that the predictions of the amplitude, the spectral index and tensor modes can be affected when another source of fluctuations is introduced in the model. Interestingly, some models of inflation which are disfavored by the data can be liberated by assuming the curvaton mechanism to work because of such modifications [9, 10, 11, 12, 13, 14, 15, 16]. In particular, in Ref. [15], it has been studied in what cases models of inflation can be relaxed by adding fluctuations from the curvaton in some

detail assuming some concrete inflation models focusing on the spectral index and the tensor-to-scalar ratio. In any case, since we can expect much more precise measurements of these quantities in the future experiment such as Planck, we should also investigate the predictions for the scale dependence of primordial curvature fluctuations and tensor modes in the mixed scenario as well as that for non-Gaussianity. Another aim of this paper is to analyze this issue extending the work of Ref. [15] to include the case where the curvaton is always subdominant component in the history of the universe, which was not considered in Ref. [15]. Then we study the effects of the curvaton on inflationary parameters such as the spectral index and the tensor-to-scalar ratio and compare with recent observations of WMAP. Furthermore, we also discuss in what cases/models large non-Gaussianity can be generated satisfying the constraints on the scale dependence and tensor modes of primordial fluctuations in the scenario.

The structure of this paper is as follows. In the next section, we discuss the formalism to study observational quantities in models with mixed fluctuations from the inflaton and the curvaton. We derive the expressions for the scalar spectral index, its running, the tensor-to-scalar ratio and the non-linearity parameters for such mixed models. Then, in Section 3, we investigate those inflationary parameters assuming several concrete inflation models. First of all, we study the scalar spectral index and the tensor-to-scalar ratio for each model and then discuss whether they are compatible with current observations. For inflation models which are considered to have been already excluded by the data, we discuss in what case the curvaton can liberate the model. Specifically, we discuss in what cases non-Gaussianity can be large. The final section is devoted to conclusion and summary of this paper.

2 Formalism

2.1 δN formalism and some definitions

In the following, we adopt the δN formalism [17, 18, 19, 20] to calculate the primordial power spectrum and some non-linearity parameters. Thus we briefly review the δN formalism here.

In the δN formalism, the primordial curvature perturbation ζ on the uniform energy density hypersurface at the time $t = t_f$ is equal to the perturbation in the local expansion defined with respect to an initial spatially flat hypersurface. On sufficiently large scales where the spatial gradient can be neglected, the local expansion is well approximated by the expansion of the unperturbed universe,

$$N(t_*, t_f, x) = \int_{t_*}^{t_f} H(x, t) dt. \quad (1)$$

where H is the local Hubble expansion and t_* is some time during inflation. Then the primordial curvature perturbation can be expressed as

$$\zeta(t_f, \vec{x}) = N(t_f, t_*, \vec{x}) - \bar{N}, \quad (2)$$

where \bar{N} is the expansion in the background spacetime:

$$\bar{N} = \int_{t_*}^{t_f} \bar{H}(t) dt. \quad (3)$$

If we take t_* as a time when the cosmological scale crossed the horizon scale during inflation, then $N(t_f, t_*, \vec{x})$ becomes a function of the scalar field at the time of horizon crossing. Hence ζ can be written as,

$$\zeta(t_f) = N_a \delta\phi_*^a + \frac{1}{2} N_{ab} \delta\phi_*^a \delta\phi_*^b + \frac{1}{6} N_{abc} \delta\phi_*^a \delta\phi_*^b \delta\phi_*^c + \dots, \quad (4)$$

where the summation is implied over repeated indices which label the scalar field. Here $\delta\phi_*^a$ is the perturbation of the scalar field ϕ^a on the flat slicing at the time of horizon crossing. In the following, when the asterisk $*$ is shown in the subscript, it indicates that the quantities are evaluated at the time of horizon crossing. N_a , N_{ab} , and N_{abc} are given by

$$N_a \equiv \frac{\partial N}{\partial \phi^a}, \quad N_{ab} \equiv \frac{\partial^2 N}{\partial \phi^a \partial \phi^b}, \quad N_{abc} \equiv \frac{\partial^3 N}{\partial \phi^a \partial \phi^b \partial \phi^c}. \quad (5)$$

For the purpose of this paper, we include the terms up to cubic order in the perturbations of the scalar field. If we choose t_f well after the reheating, then $\zeta(t_f)$ gives the primordial adiabatic perturbations.

Now we write down the expression for the primordial power spectrum which is defined as

$$\langle \zeta_{\vec{k}_1} \zeta_{\vec{k}_2} \rangle = (2\pi)^3 P_\zeta(k_1) \delta(\vec{k}_1 + \vec{k}_2). \quad (6)$$

By using Eq. (4), we can express P_ζ with the fluctuations of scalar fields as

$$P_\zeta(k) = N_a N_b P^{ab}(k), \quad (7)$$

where $P^{ab}(k)$ is the power spectrum of scalar fields:

$$\langle \delta\phi_{\vec{k}_1}^a \delta\phi_{\vec{k}_2}^b \rangle = (2\pi)^3 P^{ab}(k_1) \delta(\vec{k}_1 + \vec{k}_2). \quad (8)$$

In this paper, we consider two scalar fields, the inflaton and the curvaton which are denoted as ϕ and σ and their fluctuations are indicated as $\delta\phi$ and $\delta\sigma$ respectively. Thus the indices for scalar fields are understood to represent either of these fields in the following. The fluctuations at the time of horizon crossing $\delta\phi_*$ and $\delta\sigma_*$ are assumed to be uncorrelated random fields with the same amplitude. Hence we have

$$P^{ab}(k) = P(k) \delta^{ab} = \frac{2\pi^2}{k^3} \left(\frac{H_*}{2\pi} \right)^2 \delta^{ab}. \quad (9)$$

Then at leading order in fluctuations of the scalar fields, the power spectrum can be written as

$$P_\zeta(k) = \frac{2\pi^2}{k^3} \mathcal{P}_\zeta(k) = N_a N^a \frac{2\pi^2}{k^3} \left(\frac{H_*}{2\pi} \right)^2. \quad (10)$$

The expression for N_a will be discussed in the next subsection.

Now we discuss quantities which represent non-Gaussianity, the bispectrum and trispectrum. The definition of the bispectrum B_ζ is given by

$$\langle \zeta_{\vec{k}_1} \zeta_{\vec{k}_2} \zeta_{\vec{k}_3} \rangle = (2\pi)^3 B_\zeta(k_1, k_2, k_3) \delta(\vec{k}_1 + \vec{k}_2 + \vec{k}_3). \quad (11)$$

As is the case with the power spectrum, the leading order bispectrum can be written as

$$B_\zeta(k_1, k_2, k_3) = N_a N_b N_c B^{abc}(k_1, k_2, k_3) + N_a N_b N_c N_d (P^{ac}(k_1) P^{bd}(k_2) + P^{ac}(k_2) P^{bd}(k_3) + P^{ac}(k_3) P^{bd}(k_1)), \quad (12)$$

where B^{abc} is the bispectrum of the scalar fields

$$\langle \delta\phi_{\vec{k}_1}^a \delta\phi_{\vec{k}_2}^b \delta\phi_{\vec{k}_3}^c \rangle = (2\pi)^3 B^{abc}(k_1, k_2, k_3) \delta(\vec{k}_1 + \vec{k}_2 + \vec{k}_3). \quad (13)$$

The trispectrum T_ζ is defined as

$$\langle \zeta_{\vec{k}_1} \zeta_{\vec{k}_2} \zeta_{\vec{k}_3} \zeta_{\vec{k}_4} \rangle = (2\pi)^3 T_\zeta(k_1, k_2, k_3, k_4) \delta(\vec{k}_1 + \vec{k}_2 + \vec{k}_3 + \vec{k}_4), \quad (14)$$

and can be given with the power spectrum P^{ab} , the bispectrum B^{abc} and the trispectrum T^{abcd} for the scalar fields,

$$T_\zeta(k_1, k_2, k_3, k_4) = N_a N_b N_c N_d T^{abcd}(k_1, k_2, k_3, k_4) + N_{ab} N_c N_d N_e (P^{ac}(k_1) B^{bde}(k_{12}, k_3, k_4) + 11 \text{ perms.}) + N_{ab} N_{cd} N_e N_f (P^{bd}(k_{13}) P^{ae}(k_3) P^{cf}(k_4) + 11 \text{ perms.}) + N_{abc} N_d N_e N_f (P^{ad}(k_2) P^{be}(k_3) P^{cf}(k_4) + 3 \text{ perms.}), \quad (15)$$

where $k_{ij} = |k_i + k_j|$ and T^{abcd} is given by

$$\langle \delta\phi_{\vec{k}_1}^a \delta\phi_{\vec{k}_2}^b \delta\phi_{\vec{k}_3}^c \delta\phi_{\vec{k}_4}^d \rangle = (2\pi)^3 T^{abcd}(k_1, k_2, k_3, k_4) \delta(\vec{k}_1 + \vec{k}_2 + \vec{k}_3 + \vec{k}_4). \quad (16)$$

Expressions for B_{abc} and T_{abcd} were provided in [21] and [22] for general multiple-fields slow-roll inflation (see also [23]). In the following, we will neglect B_{abc} and T_{abcd} because the inclusion of these terms only gives corrections of slow-roll order to the primordial bispectrum and trispectrum, which are far below the observational sensitivity expected for the Planck satellite. Then B_ζ and T_ζ can be written as

$$B_\zeta(k_1, k_2, k_3) = \frac{6}{5} f_{\text{NL}} (P_\zeta(k_1) P_\zeta(k_2) + P_\zeta(k_2) P_\zeta(k_3) + P_\zeta(k_3) P_\zeta(k_1)), \quad (17)$$

$$T_\zeta(k_1, k_2, k_3, k_4) = \tau_{\text{NL}} (P_\zeta(k_{13}) P_\zeta(k_3) P_\zeta(k_4) + 11 \text{ perms.}) + \frac{54}{25} g_{\text{NL}} (P_\zeta(k_2) P_\zeta(k_3) P_\zeta(k_4) + 3 \text{ perms.}), \quad (18)$$

where f_{NL} , τ_{NL} and g_{NL} are constant parameters which are given in terms of the derivatives of the number of e -folding with respect to the scalar fields as [24, 25, 26],

$$\frac{6}{5}f_{NL} = \frac{N_a N_b N^{ab}}{(N_c N^c)^2}, \quad (19)$$

$$\tau_{NL} = \frac{N_{ab} N^{ac} N^b N_c}{(N_d N^d)^3}, \quad (20)$$

$$\frac{54}{25}g_{NL} = \frac{N_{abc} N^a N^b N^c}{(N_d N^d)^3}. \quad (21)$$

These expressions are valid for the case where B_{abc} and T_{abcd} are negligibly small. Furthermore, an interesting inequality can be obtained with the help of the Cauchy-Schwartz inequality [27]:

$$\tau_{NL} \geq \frac{36}{25}f_{NL}^2. \quad (22)$$

This inequality holds for the scenarios such as the curvaton and the modulated reheating scenarios where the leading non-Gaussianity comes from super-horizon evolution.

To calculate the primordial power spectrum and the non-linearity parameters, we need to know the number of e -folding as a function of the field value of the scalar fields, the inflaton and the curvaton, from the time when the cosmological scales crossed the horizon to the time when the universe becomes radiation-dominated connected to big bang nucleosynthesis (BBN) ^{#1}. In the next subsection, we discuss this issue in detail.

2.2 Background dynamics and the number of e -folding

Here we give an explicit expression for the number of e -folding in models with the inflaton and the curvaton. For the potential of the curvaton, we take a quadratic potential,

$$U(\sigma) = \frac{1}{2}m_\sigma^2\sigma^2, \quad (23)$$

where m_σ is the curvaton mass. We assume that the energy density of the curvaton is subdominant during inflation and at least until the time when the inflaton decays into radiation. In addition, the curvaton mass is assumed as $m_\sigma \ll H_{\text{inf}}$ with H_{inf} being the Hubble parameter during inflation. In this case, the curvaton field almost stays at the initial value during inflation. After inflation ends, the inflaton oscillates around the minimum of its potential for some time, then decays into radiation. The curvaton also begins to oscillate at around a time when $H = m_\sigma$ and decays into radiation. In the following, we assume that the curvaton decays long after the onset of the curvaton

^{#1} Since we consider the scenario with the curvaton, the universe could have experienced the dominance of radiation twice after inflation ends: radiations from the decay of inflaton and curvaton. Radiation-dominated epoch here is meant to be the radiation-dominated phase after the curvaton decay.

oscillations, which is equivalent to assume that $\Gamma_\sigma/m_\sigma \ll 1$ with Γ_σ being the decay rate of the curvaton.

Here we give a rough sketch of the thermal history of the universe in this scenario. In fact, depending on the initial amplitude of the curvaton field, the thermal history after the inflaton decay can become different. When the initial value of the curvaton σ_{in} is small enough, typically as $\sigma_{\text{in}} \ll M_{\text{pl}}$, the curvaton begins to oscillate around the minimum of the potential during radiation-dominated epoch due to the inflaton decay. With the potential Eq. (23), the energy density of the curvaton decreases as $\rho_\sigma \propto a^{-3}$ when σ oscillates. On the other hand, the energy density of radiation decreases as $\rho_{\text{rad}} \propto a^{-4}$, thus the curvaton can become dominant if the curvaton oscillates around the potential minimum long enough before decaying into radiation. If the decay rate of the curvaton is not so small, it can decay before it becomes a dominant component. In any case, when the rate of the Hubble expansion H becomes comparable to the decay rate of the curvaton, the curvaton decays into radiation. After the curvaton decays into radiation, the universe is radiation-dominated and is led to BBN epoch.

When the initial value for the curvaton field is large enough, typically as $\sigma_{\text{in}} \gg M_{\text{pl}}$, the curvaton almost stays at the initial value and drives the second inflation even after the onset of the radiation-dominated epoch due to the inflaton decay. The thermal history in this case is as follows: after the inflation driven by the inflaton ends, the inflaton decays into radiation, then the universe becomes radiation dominated. When the initial amplitude of the curvaton is large, σ stays at the initial value until long after the inflaton decays into radiation. Since the energy density of such a scalar field is constant, at some epoch, the energy density of the curvaton dominates to give the second inflationary epoch. This situation is similar to that of a double inflation model [28]. After the curvaton drives the second inflation, it begins to oscillate around the minimum of the potential when the Hubble parameter decreases as $H \sim m_\sigma$. Then the curvaton decays into radiation when $\Gamma_\sigma \sim H$.

Since we would like to calculate the primordial power spectrum and some non-linearity parameters during the radiation-dominated epoch after the curvaton decay, we need to know the e -folding number from the time when the cosmological scale exits the horizon during inflation to the time after the decay of the curvaton. We denote the number of e -folding during these epochs as N_{tot} . For later convenience, we divide N_{tot} into several parts as

$$N_{\text{tot}} = N_{\text{inf}} + N_{\text{d}} + N_{\text{R}} \quad (24)$$

where N_{inf} represents the number of e -folding during inflation driven by the inflaton. N_{d} is for the epoch from the end of inflation to some time after the decay of the inflaton. N_{R} refers to the e -folding number from that time to the time well after the curvaton decay. N_{R} is relevant to the curvaton dynamics.

Now we make detailed discussion on N_{inf} , N_{d} and N_{R} in order to calculate the primordial power spectrum and the non-linearity parameters in the δN formalism. We do not

discuss N_d here since it is irrelevant to the primordial fluctuation^{#2}. However, when we relate the cosmological scales observed today to the time of horizon exit during inflation, we also need N_d , which we will discuss in the subsection 2.6.

First we start with N_{inf} , the number of e -folding during inflation. It is determined by the dynamics of the inflaton whose equation of motion is

$$\ddot{\phi} + 3H\dot{\phi} + V_\phi = 0, \quad (25)$$

where a dot represents the derivative with respect to the cosmic time and $V_\phi = dV/d\phi$. During the inflation, the so-called slow-roll (SR) approximation is valid. Hence N_{inf} can be written as, by using $\dot{\phi} \simeq -V_\phi/(3H)$,

$$N_{\text{inf}} = \int_{t_*}^{t_e} H dt \simeq -\frac{1}{M_{\text{pl}}^2} \int_{\phi_*}^{\phi_e} \frac{V}{V_\phi} d\phi \quad (26)$$

where t_* and t_e respectively represent the times when a scale exits the horizon and when the inflation ends. Similarly, ϕ_* and ϕ_e indicate the scalar field values at corresponding epochs. To give a more concrete expression for N_{inf} , we need to specify the potential for the inflaton.

Next we consider N_{R} . After the inflaton decays into the radiation, the universe is composed of radiation and the curvaton. Hence the background equations are given by

$$\dot{\rho}_r + 4H\rho_r = \Gamma_\sigma \rho_\sigma, \quad (27)$$

$$\ddot{\sigma} + (3H + \Gamma_\sigma)\dot{\sigma} + m_\sigma^2 \sigma = 0, \quad (28)$$

$$H^2 = \frac{1}{3M_{\text{pl}}^2}(\rho_r + \rho_\sigma), \quad (29)$$

where ρ_r and $\rho_\sigma = (1/2)\dot{\sigma}^2 + U(\sigma)$ are energy densities of radiation and the curvaton, respectively. To obtain N_{R} , we solve the above equations from the time $t = t_0$ which corresponds to some time after the reheating epoch due to the decay of the inflaton with the initial conditions

$$\rho_r(t_0) = \rho_{r0}, \quad \sigma(t_0) = \sigma_*, \quad \dot{\sigma}(t_0) \simeq -\frac{m_\sigma^2 \sigma_*}{3H(t_0)}, \quad (30)$$

to the time t_f when the Hubble parameter becomes much smaller than Γ_σ , i.e., $H(t_f) \ll \Gamma_\sigma$. Here we denote the initial amplitude for the curvaton field with an asterisk as σ_* . Remind that we are using an asterisk to represent that a quantity is evaluated at the time of horizon exit. Since σ almost stays at the initial position during inflation, the initial value

^{#2} In the case that the curvaton energy density becomes dominant during the regime of the inflaton oscillations, N_d depends on σ_* so that it is also relevant to the primordial fluctuations. However, as stated in the paragraph below Eq. (23), we do not consider such a case in this paper.

for σ here is the same as that at the horizon exit during inflation. By integrating Eq. (27), we can write N_R formally as

$$N_R = \frac{1}{4} \log \frac{\rho_{r0}}{\rho_f} + \frac{1}{4} \log (1 + F(\sigma_*, m_\sigma, \Gamma_\sigma)), \quad (31)$$

where $F(\sigma_*, m_\sigma, \Gamma_\sigma)$ is defined as

$$F(\sigma_*, m_\sigma, \Gamma_\sigma) \equiv \int_0^\infty dN e^{4N} \frac{\Gamma_\sigma}{H(N)} \frac{\rho_\sigma(N)}{\rho_{r0}}, \quad (32)$$

and $\rho_f = \rho_r(t_f)$. In general, we need a numerical calculation to evaluate $F(\sigma_*, m_\sigma, \Gamma_\sigma)$. However, for some cases, we can integrate analytically the right hand side (RHS) of Eq. (32), which will be explicitly given in the next subsection. It should be noted here that, when the curvaton does not drive the secondary inflation and begins to oscillate during the radiation-dominated epoch caused by the inflaton decay, the value of F depends only on the combination

$$p \equiv \frac{\sigma_*^2}{M_{\text{pl}}^2 \sqrt{\Gamma_\sigma/m_\sigma}}. \quad (33)$$

When the curvaton is oscillating, it can be regarded as a matter fluid as long as the background evolution is concerned. Then the universe can be regarded as a two component system which consists of matter and radiation. In this case, it has been shown that the solution for the system of Eqs. (27), (28) and (29) depends only on the single parameter p defined above [29]. Thus F can be determined once p is fixed for such a case.

When the second inflation driven by the curvaton occurs, the curvaton cannot be regarded as matter. However, even in this case, the value of F can be determined once σ_* and the combination Γ_σ/m_σ are given. During the second inflationary phase, the slow-roll approximation is valid for the curvaton field as in the case during inflation. In this case, N_R can be written as

$$N_R \simeq -\frac{1}{M_{\text{pl}}^2} \int_{\sigma_*}^{\sigma_{\text{end}}} \frac{U}{U_\sigma} d\sigma + C, \quad (34)$$

where σ_{end} is the value of σ at the end of the second inflation. C represents the e -folding number from the end of the second inflation to the time well after the curvaton decay and does not depend on σ_* . Thus, even in this case, once the combination Γ_σ/m_σ is given along with σ_* , the number of e -folding N_R is determined. Hence, we define the combination of the variables as

$$s \equiv \frac{\Gamma_\sigma}{m_\sigma}, \quad (35)$$

which will be used frequently instead of giving Γ_σ and m_σ separately. As stated before, we assume $s \ll 1$ in this paper.

Having described the necessary formulae in the δN formalism, we discuss primordial curvature fluctuations, tensor modes and non-Gaussianity in the following subsections.

2.3 Primordial power spectrum

Now we discuss primordial power spectrum in models with mixed fluctuations from the inflaton and the curvaton. By using the δN formalism, the primordial curvature perturbation ζ can be calculated as

$$\zeta \simeq \frac{1}{M_{\text{pl}}^2} \frac{V}{V_\phi} \delta\phi_* + \frac{\partial Q}{\partial \sigma} \delta\sigma_*, \quad (36)$$

where Q represents the σ_* dependent part of N_{R} which is defined as

$$Q \equiv \frac{1}{4} \log(1 + F). \quad (37)$$

In actual calculations, we numerically obtain the function F in all cases. The primordial power spectrum for a model with mixed inflaton and curvaton fluctuations is given as

$$\mathcal{P}_\zeta = \left(\frac{1}{M_{\text{pl}}^4} \frac{V^2}{V_\phi^2} + Q_\sigma^2 \right) \left(\frac{H}{2\pi} \right)^2, \quad (38)$$

where $Q_\sigma \equiv \partial Q / \partial \sigma$ and we used Eq. (9). The spectral index and its running are given by

$$\begin{aligned} n_s - 1 &\equiv \left. \frac{d \log \mathcal{P}_\zeta}{d \log k} \right|_{k=aH} \\ &= -2\epsilon - \frac{4\epsilon - 2\eta}{1 + 2\epsilon M_{\text{pl}}^2 Q_\sigma^2}, \end{aligned} \quad (39)$$

$$\begin{aligned} n_{\text{run}} &\equiv \frac{dn_s}{d \log k} \\ &= -4\epsilon(2\epsilon - \eta) - \frac{2}{(1 + 2\epsilon M_{\text{pl}}^2 Q_\sigma^2)^2} [8\epsilon^2 - 6\epsilon\eta + \xi^2 + 2\epsilon(2\epsilon\eta - 2\eta^2 + \xi^2)M_{\text{pl}}^2 Q_\sigma^2], \end{aligned} \quad (40)$$

where ϵ, η and ξ^2 are the slow-roll parameters which are defined as

$$\epsilon \equiv \frac{1}{2} M_{\text{pl}}^2 \left(\frac{V_\phi}{V} \right)^2, \quad \eta \equiv M_{\text{pl}}^2 \frac{V_{\phi\phi}}{V}, \quad \xi^2 \equiv M_{\text{pl}}^4 \frac{V_\phi V_{\phi\phi\phi}}{V^2}. \quad (41)$$

Here the third parameter ξ^2 should be considered to be the second order in the slow-roll.

During inflation, tensor modes are also generated as

$$\mathcal{P}_T = \frac{8}{M_{\text{pl}}^2} \left(\frac{H}{2\pi} \right)^2. \quad (42)$$

When one extracts the information on tensor modes, the tensor-to-scalar ratio is usually used, which is defined and given in the case considered here as

$$r \equiv \frac{\mathcal{P}_T}{\mathcal{P}_\zeta} = \frac{16\epsilon}{1 + 2\epsilon M_{\text{pl}}^2 Q_\sigma^2}. \quad (43)$$

In the pure curvaton limit, $2\epsilon M_{\text{pl}}^2 Q_\sigma^2 \gg 1$, where the primordial fluctuations are completely dominated by the curvaton fluctuations, n_s , n_{run} and r reduce to

$$n_s - 1 = -2\epsilon, \quad (44)$$

$$n_{\text{run}} = -4\epsilon(2\epsilon - \eta), \quad (45)$$

$$r = \frac{8}{M_{\text{pl}}^2 Q_\sigma^2}. \quad (46)$$

We find that the spectrum of the scalar fluctuations becomes red-tilted, the running of the spectral index becomes independent of ξ^2 , and the tensor-to-scalar ratio becomes negligible.

2.4 Non-linearity parameters

In the subsection 2.1, we gave the definitions of non-linearity parameters of f_{NL} , τ_{NL} and g_{NL} in the δN formalism. Here we give concrete expressions for them in models with mixed fluctuations from the inflaton and the curvaton.

To obtain the bispectrum and the trispectrum, we need to expand δN up to cubic order in $\delta\phi$ and $\delta\sigma$, which can be written as

$$\begin{aligned} \zeta \simeq \frac{V}{V_\phi} \delta\phi_* + \frac{1}{2} \left(1 - \frac{VV_{\phi\phi}}{V_\phi^2} \right) \delta\phi_*^2 - \frac{V_{\phi\phi}}{6V_\phi} \left(1 + \frac{VV_{\phi\phi\phi}}{V_\phi V_{\phi\phi}} - \frac{2VV_{\phi\phi}}{V_\phi^2} \right) \delta\phi_*^3 \\ + Q_\sigma \delta\sigma_* + \frac{1}{2} Q_{\sigma\sigma} \delta\sigma_*^2 + \frac{1}{6} Q_{\sigma\sigma\sigma} \delta\sigma_*^3. \end{aligned} \quad (47)$$

Then, using Eqs. (19), (20) and (21), the non-linearity parameters are given by

$$\frac{6}{5} f_{\text{NL}} = \frac{1}{(1 + 2\epsilon M_{\text{pl}}^2 Q_\sigma^2)^2} [2\epsilon - \eta + 4\epsilon^2 M_{\text{pl}}^4 Q_\sigma^2 Q_{\sigma\sigma}], \quad (48)$$

$$\tau_{\text{NL}} = \frac{1}{(1 + 2\epsilon M_{\text{pl}}^2 Q_\sigma^2)^3} [(2\epsilon - \eta)^2 + 8\epsilon^3 M_{\text{pl}}^6 Q_\sigma^2 Q_{\sigma\sigma}^2], \quad (49)$$

$$\frac{54}{25} g_{\text{NL}} = \frac{1}{(1 + 2\epsilon M_{\text{pl}}^2 Q_\sigma^2)^3} [-2\epsilon\eta - \xi^2 + 2\eta^2 + 8\epsilon^3 M_{\text{pl}}^6 Q_\sigma^3 Q_{\sigma\sigma\sigma}]. \quad (50)$$

In the pure curvaton limit, $2\epsilon M_{\text{pl}}^2 Q_\sigma^2 \gg 1$, these expressions reduce to

$$\frac{6}{5} f_{\text{NL}} = \frac{Q_{\sigma\sigma}}{Q_\sigma^2}, \quad (51)$$

$$\tau_{\text{NL}} = \frac{Q_{\sigma\sigma}^2}{Q_\sigma^4} = \frac{36}{25} f_{\text{NL}}^2, \quad (52)$$

$$\frac{54}{25} g_{\text{NL}} = \frac{Q_{\sigma\sigma\sigma}}{Q_\sigma^3}. \quad (53)$$

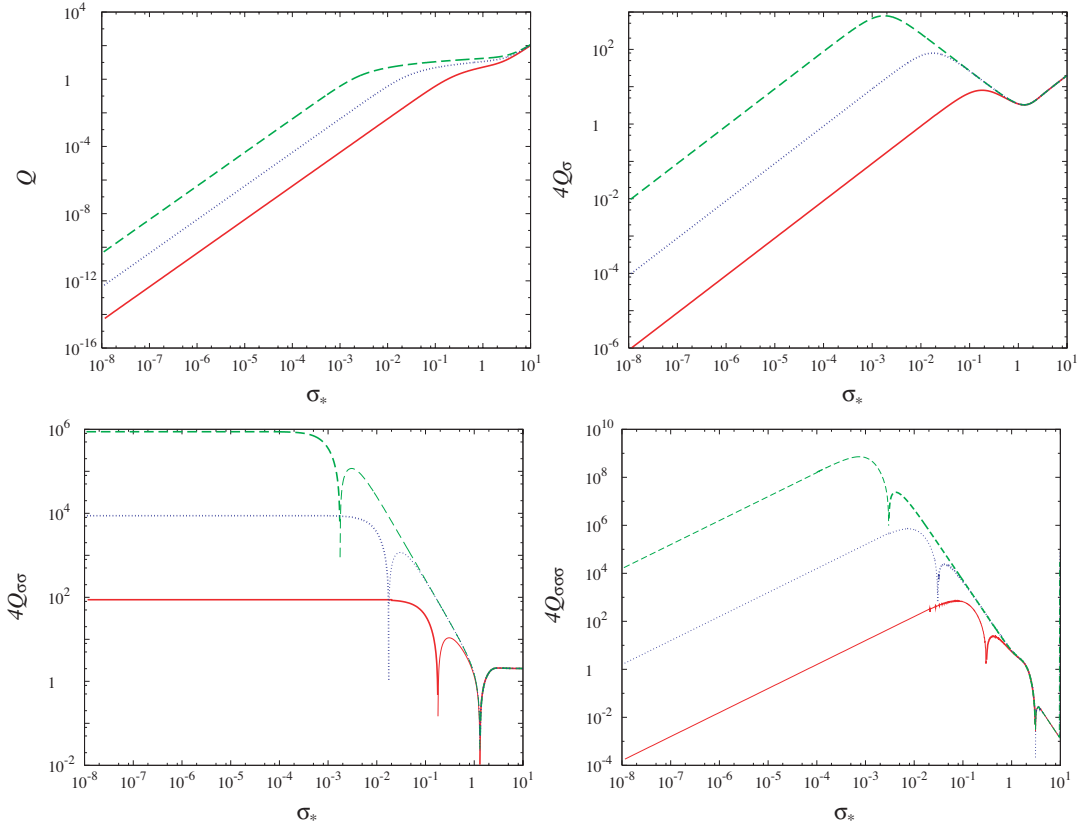


Figure 1: Plots of Q (top left), Q_σ , (top right), $Q_{\sigma\sigma}$ (bottom right) and $Q_{\sigma\sigma\sigma}$ (bottom left) as functions of σ_* for the cases with $s = 10^{-4}$ (red solid line), $s = 10^{-8}$ (blue dotted line) and $s = 10^{-12}$ (green dashed line). Notice that $Q_{\sigma\sigma}$ and $Q_{\sigma\sigma\sigma}$ can be negative. When the functions take a negative value, the absolute value is drawn with a thin line. σ_* is shown in units of M_{pl} .

Once we pick up a model of inflation and calculate the values of Q_σ , $Q_{\sigma\sigma}$ and $Q_{\sigma\sigma\sigma}$, we can give concrete values for these non-linearity parameters along with n_s and r . Although an analytic expression can be obtained for some limiting values of p and σ_* , which is going to be discussed in the next subsection, a numerical calculation is needed to evaluate Q_σ , $Q_{\sigma\sigma}$ and $Q_{\sigma\sigma\sigma}$ in general. In Fig. 1, we show them as functions of σ_* for several values of s . From the figure, we can obtain some idea of when the contribution from the curvaton significantly affects the primordial power spectrum and non-Gaussianity.

2.5 Analytic expressions in limiting cases

As previously mentioned, the value of F can be obtained by numerical calculations in general. However, we can express it analytically in some limiting cases. In the following, we

begin with the case where the initial amplitude of the curvaton σ_* is very small ($\sigma_* \ll M_{\text{pl}}$). In fact, this case can be further divided into two situations. The first case is that energy density of the curvaton once dominates the universe before the decay of the curvaton. The other case is that it can be always neglected compared to radiation during the whole history of the universe. These two cases correspond to $p \gg 1$ and $p \ll 1$, respectively. After discussing these cases, we consider the situation where the initial amplitude for the curvaton is large enough to drive the second inflation. Now we look at these cases in order.

2.5.1 The case with $\sigma_* \ll M_{\text{pl}}$ and $p \gg 1$

Here we adopt the so-called sudden decay approximation, which can give a good description for the case with $p \gg 1$. In this approximation, the curvaton decays suddenly when $H = \Gamma_\sigma$ at $N = N_d$. That is, we shall regard energy densities ρ_r and ρ_σ to behave like the step functions at the time of the curvaton decay. All ρ_σ is transferred to ρ_r . Hence ρ_r increases by ρ_σ at the time of the curvaton decay. Then, the equation for radiation energy density is written as

$$\frac{d\rho_r}{dN} + 4\rho_r = \rho_\sigma(N_{d-})\delta(N - N_d), \quad (54)$$

where the equation is written in terms of the derivative with respect to the number of e -folding and N_{d-} represents an e -folding number just before the time when $H = \Gamma_\sigma$. The coefficient on the RHS is chosen so that the total energy density is conserved through the curvaton decay. Then, the equation corresponding to Eq. (32) can be written as

$$F(\sigma_*, m_\sigma, \Gamma_\sigma) = \frac{\rho_\sigma(N_{d-})}{\rho_r(N_{d-})}. \quad (55)$$

Now let us introduce a new quantity q defined as

$$q \equiv \frac{3\rho_\sigma(N_{d-})}{4\rho_r(N_{d-}) + 3\rho_\sigma(N_{d-})}, \quad (56)$$

which roughly represents the fraction of energy density of the curvaton to the total one at the time of the curvaton decay. With this parameter q , $F(\sigma_*, m_\sigma, \Gamma_\sigma)$ can be written as

$$F(\sigma_*, m_\sigma, \Gamma_\sigma) = \frac{4}{3} \frac{q}{1 - q}. \quad (57)$$

Since we can relate q to σ_* , we can obtain the analytic expression of Q_σ as a function of σ_* , m_σ and Γ_σ . For this purpose, let us write down the relation between q and σ_* in a following way. The Friedman equation at the time of the curvaton decay is given by

$$H^2(N_d) = \Gamma_\sigma^2 = \frac{1}{3M_{\text{pl}}^2} \left(\rho_r(N_{d-}) + \rho_\sigma(N_{d-}) \right). \quad (58)$$

Denoting the e -folding number at the time $H = m_\sigma$ as N_m , this equation can be written as

$$\Gamma_\sigma^2 = \frac{1}{3M_{\text{pl}}^2} \left(3m_\sigma^2 M_{\text{pl}}^2 e^{-4\bar{N}} + \rho_\sigma(N_m) e^{-3\bar{N}} \right), \quad (59)$$

where $\bar{N} = N_d - N_m$. Furthermore, by using the relation

$$\frac{\rho_\sigma(N_m)}{3m_\sigma^2 M_{\text{pl}}^2} e^{\bar{N}} = \frac{\rho_\sigma(N_{d-})}{\rho_r(N_{d-})} = \frac{4}{3} \frac{q}{1-q}, \quad (60)$$

one can relate q and $\rho_\sigma(N_m)$ as:

$$\frac{\Gamma_\sigma}{m_\sigma} = \frac{1}{16} \left(\frac{\rho_\sigma(N_m)}{m_\sigma^2 M_{\text{pl}}^2} \right)^2 \frac{(3+q)^{1/2}}{3^{1/2} q^2} (1-q)^{3/2}. \quad (61)$$

Now we write the energy density of the curvaton at $N = N_m$ as $\rho_\sigma(N_m) = (1/2)m_\sigma^2 \alpha^2 \sigma_*^2$ where α parameterizes the amplitude of the curvaton at the onset of oscillations relative to the initial one. The concrete value of α is given in Appendix A. By using them, we obtain the relation between q and σ_* as

$$\alpha^2 p = \frac{3^{1/4} 8q}{(3+q)^{1/4} (1-q)^{3/4}}. \quad (62)$$

By using Eqs. (57) and (62), we obtain the expressions for the derivatives of F with respect to σ , which is necessary to evaluate the inflationary parameters, for this limiting case as

$$Q_\sigma = \frac{2}{3} \frac{q}{\sigma_*}, \quad Q_{\sigma\sigma} = \frac{2}{9} \frac{q}{\sigma_*^2} (3 - 4q - 2q^2), \quad Q_{\sigma\sigma\sigma} = \frac{4}{27} \frac{q^2}{\sigma_*^3} (-18 + q + 20q^2 + 6q^3). \quad (63)$$

In the limit $q = 1$, which is equivalent to $p \gg 1$, Q_σ becomes

$$Q_\sigma = \frac{2}{3} \frac{1}{\sigma_*}. \quad (64)$$

This agrees with the result in [14] where asymptotic form of Q_σ for $\sigma_* \ll M_{\text{pl}}$ is provided under the assumption that curvaton once dominates the universe before the curvaton decays. Hence the sudden decay approximation can well describe Q for the case $p \gg 1$.

Using Eq. (63), the non-linearity parameters for $p \gg 1$ can be written as

$$\frac{6}{5} f_{\text{NL}} = \frac{1}{\left(1 + \frac{8}{9} \epsilon \frac{M_{\text{pl}}^2}{\sigma_*^2}\right)^2} \left(2\epsilon - \eta - \frac{32}{27} \epsilon^2 \frac{M_{\text{pl}}^4}{\sigma_*^4} \right), \quad (65)$$

$$\tau_{\text{NL}} = \frac{1}{\left(1 + \frac{8}{9} \epsilon \frac{M_{\text{pl}}^2}{\sigma_*^2}\right)^3} \left\{ (2\epsilon - \eta)^2 + \frac{128}{81} \epsilon^3 \frac{M_{\text{pl}}^6}{\sigma_*^6} \right\}, \quad (66)$$

$$\frac{54}{25} g_{\text{NL}} = \frac{1}{\left(1 + \frac{8}{9} \epsilon \frac{M_{\text{pl}}^2}{\sigma_*^2}\right)^3} \left(-2\epsilon\eta - \xi^2 + 2\eta^2 + \frac{256}{81} \epsilon^3 \frac{M_{\text{pl}}^6}{\sigma_*^6} \right). \quad (67)$$

All the magnitudes of these non-linearity parameters become the largest when $\sigma_* \sim \sqrt{\epsilon} M_{\text{pl}}$. Substituting $\sigma_* = \sqrt{\epsilon} M_{\text{pl}}$ to the equations above, we find that the maximum magnitudes of f_{NL} , τ_{NL} and g_{NL} are all $\mathcal{O}(1)$. Hence large non-Gaussianity is not produced for $p \gg 1$.

2.5.2 The case with $\sigma_* \ll M_{\text{pl}}$ and $p \ll 1$

Now we consider the second case where the curvaton is always subdominant in the history of the universe. Even in this case, the sudden decay approximation adopted above can give a good estimate to some extent, but its accuracy is $\mathcal{O}(10\%)$ compared to numerical calculations^{#3}. However, another approach can give a better analytic expression for Q . Detailed descriptions for the derivation of the analytic formulae can be found in Appendix B. Here we just give the expressions.

Since here we are considering the case with $p \ll 1$, we expand F up to the second order in p , which is necessary for obtaining the formula for the third derivative of Q with respect to σ because the third derivative of p with respect to σ vanishes. After some calculations, we can show that the function F can be expanded as

$$F(p) = \frac{1}{6} \sqrt{\frac{\pi}{2}} \alpha^2 p + \frac{1}{144} \alpha^4 p^2 + \mathcal{O}(p^3), \quad (68)$$

where we neglected higher order terms in s assuming $s \ll 1$. Thus the derivatives of Q with respect to σ are given for this case as

$$Q_\sigma = \frac{1}{12} \sqrt{\frac{\pi}{2}} \alpha^2 \frac{\sigma_*}{M_{\text{pl}}^2 \sqrt{s}} (1 + \mathcal{O}(p)), \quad (69)$$

$$Q_{\sigma\sigma} = \frac{1}{12} \sqrt{\frac{\pi}{2}} \alpha^2 \frac{1}{M_{\text{pl}}^2 \sqrt{s}} (1 + \mathcal{O}(p)), \quad (70)$$

$$Q_{\sigma\sigma\sigma} = -\frac{1}{24} (\pi - 1) \alpha^4 \frac{\sigma_*}{M_{\text{pl}}^4 s} (1 + \mathcal{O}(p)). \quad (71)$$

Here notice that, while Q_σ and $Q_{\sigma\sigma}$ come from the leading order term in p , $Q_{\sigma\sigma\sigma}$ comes from the next-to-leading order term in p . With the expressions above, we can explicitly write down the non-linearity parameters as:

$$\frac{6}{5} f_{\text{NL}} = \frac{1}{6} \sqrt{\frac{\pi}{2}} \alpha^2 \frac{\epsilon}{\sqrt{s}} D_f \left(\frac{\pi \alpha^4}{144} \epsilon \frac{p}{\sqrt{s}} \right) (1 + \mathcal{O}(p)), \quad (72)$$

$$\tau_{\text{NL}} = \left(\frac{1}{6} \sqrt{\frac{\pi}{2}} \alpha^2 \frac{\epsilon}{\sqrt{s}} \right)^2 D_\tau \left(\frac{\pi \alpha^4}{144} \epsilon \frac{p}{\sqrt{s}} \right) (1 + \mathcal{O}(p)), \quad (73)$$

$$\frac{54}{25} g_{\text{NL}} = -(\pi - 1) \sqrt{\frac{2}{\pi}} \alpha^2 \frac{\epsilon}{\sqrt{s}} D_g \left(\frac{\pi \alpha^4}{144} \epsilon \frac{p}{\sqrt{s}} \right) (1 + \mathcal{O}(p)), \quad (74)$$

^{#3} Using the fitting formula, the sudden-decay approximation can give an accurate estimate for some parameter range [30].

where the functions D_f, D_τ and D_g are defined as

$$D_f(x) \equiv \frac{x}{(1+x)^2}, \quad D_\tau(x) \equiv \frac{x}{(1+x)^3}, \quad D_g(x) \equiv \frac{x^2}{(1+x)^3}. \quad (75)$$

In deriving these expressions, we have neglected the non-Gaussianity coming from the inflaton fluctuations because they are small quantities. In the pure curvaton limit, the non-linearity parameters given above become

$$\frac{6}{5}f_{\text{NL}} = \frac{24}{\sqrt{2\pi}\alpha^2} \frac{1}{p}, \quad \tau_{\text{NL}} = \frac{288}{\pi\alpha^4} \frac{1}{p^2}, \quad \frac{54}{25}g_{\text{NL}} = -\frac{288(\pi-1)}{\sqrt{2\pi^3}\alpha^2} \frac{1}{p}. \quad (76)$$

Using Eqs. (72), (73) and (74), we can derive a relation among the non-linearity parameters specific to this case (i.e., $p \ll 1$). After a little arithmetic, we obtain

$$-\frac{5\pi}{48(\pi-1)} \frac{\tau_{\text{NL}}g_{\text{NL}}}{f_{\text{NL}}^3} = 1 + \mathcal{O}(p). \quad (77)$$

When $p \ll 1$, p can be written using f_{NL} and τ_{NL} as

$$p = \sqrt{\frac{\pi}{2}} \frac{5184}{125\alpha^2} f_{\text{NL}}^{-1} \left(\frac{f_{\text{NL}}^2}{\tau_{\text{NL}}} \right)^2 = \mathcal{O} \left(f_{\text{NL}}^{-1} \left(\frac{f_{\text{NL}}^2}{\tau_{\text{NL}}} \right)^2 \right). \quad (78)$$

Because of the inequality Eq. (22), the magnitude of p is smaller than that of f_{NL}^{-1} . Hence for the case of the very large non-Gaussianity ($f_{\text{NL}} \gg 1$) which occurs only when $p \ll 1$, the RHS in Eq. (77) becomes very close to unity and the equation provides a simple consistency relation between the bispectrum and the trispectrum. Note that this relation holds not only for the pure curvaton model but also for the mixed model of the inflaton and the curvaton. Neglecting the second term on the RHS in Eq. (77), we can further derive the inequality for f_{NL} and g_{NL} as, assuming f_{NL} being positive,

$$g_{\text{NL}} \leq -\frac{20(\pi-1)}{3\pi} f_{\text{NL}}. \quad (79)$$

Thus if the very large non-Gaussianity is detected in the future, we can discriminate the mixed model of the inflaton and the curvaton from other scenarios that also generate large non-Gaussianity by using these consistency relations.

Furthermore, notice that the argument x of the functions D_f, D_τ and D_g corresponds to the ratio of the inflaton's fluctuation to the curvaton's, i.e., $x = 2\epsilon M_{\text{pl}}^2 Q_\sigma^2 = \zeta_{\text{cur}}^2 / \zeta_{\text{inf}}^2$ where ζ_{inf} and ζ_{cur} are the curvature fluctuations generated from the inflaton and the curvaton respectively. Since all these functions take the maximum values at $x \sim 1$, non-linearity parameters become the largest when the fluctuations from the curvaton are comparable to those generated from the inflaton with ϵ and s being fixed. In this case, the initial amplitude of the curvaton becomes $\sigma_* \sim \sigma_{*,\text{max}} \sim \sqrt{s/\epsilon} M_{\text{pl}}$. If σ_* is smaller than $\sigma_{*,\text{max}}$, the curvature perturbations are dominated by the inflaton fluctuations which are highly

Gaussian. Hence when σ_* is smaller than $\sigma_{*,\max}$, the magnitudes of the non-linearity parameters take smaller values. On the other hand, if σ_* is larger than $\sigma_{*,\max}$, it becomes similar to the pure curvaton case, in which fluctuations from the curvaton dominate over those of the inflaton. In this case, f_{NL} and g_{NL} are proportional to $1/\sigma_*^2$ and τ_{NL} are proportional to $1/\sigma_*^4$. Hence, as we take the value of σ_* be larger than $\sigma_{*,\max}$, the magnitude of the non-linearity parameters becomes smaller. Thus if we vary σ_* under the condition that ϵ and s are fixed, in which we are changing the amplitude of ζ_{cur} with ζ_{inf} being fixed, the non-Gaussianity becomes the largest when $\sigma_* \sim \sigma_{*,\max}$, i.e., when the contributions from the inflaton and the curvaton are comparable. On the other hand, if we instead vary ϵ under the condition that s and σ_* are fixed, where we are changing the amplitude of ζ_{inf} with ζ_{cur} being fixed, the non-Gaussianity becomes the largest when the contributions from the inflaton are absent.

The maximum values of f_{NL} , τ_{NL} and the minimum value of g_{NL} for the variation of σ_* are given by

$$\frac{6}{5}f_{\text{NL},\max} = \frac{1}{24}\sqrt{\frac{\pi}{2}}\alpha^2\frac{\epsilon}{\sqrt{s}} \sim \frac{1}{p_{\max}}, \quad (80)$$

$$\tau_{\text{NL},\max} = \frac{\pi\alpha^4\epsilon^2}{486s} \sim \frac{1}{p_{\max}^2}, \quad (81)$$

$$\frac{54}{25}g_{\text{NL},\min} = -\frac{4(\pi-1)}{27}\sqrt{\frac{\pi}{2}}\alpha^2\frac{\epsilon}{\sqrt{s}} \sim \frac{1}{p_{\max}}, \quad (82)$$

where p_{\max} is the value of p with $\sigma_* = \sigma_{*,\max}$, which is much smaller than 1. We find that the magnitudes of these non-linearity parameters have the same p dependence as those in the case of the pure curvaton, i.e., f_{NL} and g_{NL} are roughly given by the inverse of the fraction of the curvaton energy density to the total one at the time of the curvaton decay and τ_{NL} is roughly given by f_{NL}^2 ^{#4}.

As a final remark of this subsection, we comment on the relation $\tau_{\text{NL}} \sim f_{\text{NL}}^2$ which holds for $\sigma_* = \sigma_{*,\max}$. In fact, this relation breaks down when σ_* deviates from $\sigma_{*,\max}$. From Eq. (75), we have

$$\frac{D_\tau(x)}{D_f^2(x)} = 1 + \frac{1}{x}. \quad (83)$$

Hence when the curvaton contribution to the curvature perturbations is subdominant, i.e., $x \ll 1$, τ_{NL} is enhanced by a factor of x^{-1} compared with f_{NL}^2 . This shows that the trispectrum as well as the bispectrum could also be important in detecting the non-Gaussianity of the primordial perturbations. As we will see in Section 3 where f_{NL} , g_{NL} and τ_{NL} are calculated for various inflation models in the mixed inflaton and curvaton

^{#4} In Ref. [31], by requiring that the homogeneous energy density of the curvaton should be larger than its gradient energy density and the decay rate Γ_σ is at least of order that given by the gravitational strength, an upper bound on f_{NL} was provided as a function of the tensor-to-scalar ratio in the pure curvaton case.

scenario, there are parameter regions where $f_{\text{NL}}, g_{\text{NL}} \lesssim \mathcal{O}(1)$ but $\tau_{\text{NL}} \gg 1$. In such a case, the leading non-Gaussianity comes not from the bispectrum but from the trispectrum through the τ_{NL} terms.

2.5.3 The case with $\sigma_* \gg M_{\text{pl}}$

When the initial amplitude is large enough, the curvaton field can drive the second inflation after the first inflation caused by the inflaton. In this case, N_{R} is calculated from Eq. (34) and is given by

$$N_{\text{R}} \simeq \frac{1}{4M_{\text{pl}}^2}(\sigma_*^2 - \sigma_e^2) + C. \quad (84)$$

Thus, in this case, Q_σ , $Q_{\sigma\sigma}$ and $Q_{\sigma\sigma\sigma}$ become

$$Q_\sigma = \frac{1}{2} \frac{\sigma_*}{M_{\text{pl}}^2}, \quad Q_{\sigma\sigma} = \frac{1}{2M_{\text{pl}}^2}, \quad Q_{\sigma\sigma\sigma} = 0. \quad (85)$$

Then, the non-linearity parameters are given by

$$\frac{6}{5}f_{\text{NL}} = \frac{1}{\left(1 + \frac{1}{2}\epsilon \frac{\sigma_*^2}{M_{\text{pl}}^2}\right)^2} \left(2\epsilon - \eta + \frac{1}{2}\epsilon^2 \frac{\sigma_*^2}{M_{\text{pl}}^2}\right), \quad (86)$$

$$\tau_{\text{NL}} = \frac{1}{\left(1 + \frac{1}{2}\epsilon \frac{\sigma_*^2}{M_{\text{pl}}^2}\right)^3} \left\{ (2\epsilon - \eta)^2 + \frac{1}{2}\epsilon^3 \frac{\sigma_*^2}{M_{\text{pl}}^2} \right\}, \quad (87)$$

$$\frac{54}{25}g_{\text{NL}} = \frac{1}{\left(1 + \frac{1}{2}\epsilon \frac{\sigma_*^2}{M_{\text{pl}}^2}\right)^3} (-2\epsilon\eta - \xi^2 + 2\eta^2). \quad (88)$$

As for f_{NL} and τ_{NL} , the contributions from the curvaton become the largest when $\sigma_* \sim M_{\text{pl}}/\sqrt{\epsilon}$. Substituting $\sigma_* \sim M_{\text{pl}}/\sqrt{\epsilon}$ to Eqs. (86) and (87), we find that the maximum contributions of the curvaton to f_{NL} and τ_{NL} are $\mathcal{O}(\epsilon)$ and $\mathcal{O}(\epsilon^2)$, respectively. As for g_{NL} , addition of the curvaton always reduces the magnitude of g_{NL} . Hence $f_{\text{NL}}, \tau_{\text{NL}}$ and g_{NL} are at most $\mathcal{O}(\epsilon, \eta), \mathcal{O}(\epsilon^2, \epsilon\eta, \eta^2)$ and $\mathcal{O}(\epsilon^2, \epsilon\eta, \eta^2, \xi^2)$, respectively.

2.6 Corresponding Scales

To compare the prediction for the primordial curvature fluctuations and non-Gaussianity with observations, we need to specify when the present cosmological scale exited the horizon during inflation. Since $k_* = a_*H_*$ holds when the scale with the wave number k_* crossed the horizon, the reference scale k_{ref} where we probe the primordial fluctuations at the present time is related to that at the horizon crossing during inflation as

$$\frac{k_{\text{ref}}}{a_0H_0} = \frac{a_*H_*}{a_0H_0}, \quad (89)$$

where a_0 and H_0 are the scale factor and the Hubble parameter at present. The ratio of a_* to a_0 in the RHS can be divided into several parts as,

$$\frac{k_{\text{ref}}}{a_0 H_0} = \frac{a_*}{a_{\text{end}}} \frac{a_{\text{end}}}{a_{\phi\text{reh}}} \frac{a_{\phi\text{reh}}}{a_f} \frac{a_f}{a_0} \frac{H_*}{H_0}. \quad (90)$$

Here a_{end} , $a_{\phi\text{reh}}$ and a_f are the scale factors at the times when the inflation driven by the inflaton ends, the inflaton decays to reheat the universe, and some time after the curvaton decays into radiation, respectively. For the definiteness, we take $H \simeq 10^{-2}\Gamma_\sigma$ as the time corresponding to a_f so that Eq. (31) gives a good description. By taking logarithm of both sides and reminding that the number of e -folding during inflation is $N_{\text{inf}} = \log(a_*/a_{\text{end}})$, N_{inf} can be written as

$$N_{\text{inf}} = -\log \frac{k_{\text{ref}}}{a_0 H_0} + \log \frac{a_{\text{end}}}{a_{\phi\text{reh}}} + \log \frac{a_{\phi\text{reh}}}{a_f} + \log \frac{a_f}{a_0} + \log \frac{H_*}{H_0}. \quad (91)$$

For the first term, we take $k_{\text{ref}} = 0.002 \text{ Mpc}^{-1}$ in the analysis. The second term in the RHS corresponds to $-N_d$ in Eq. (24), i.e., the e -folding number from the end of inflation to the decay of the inflaton to the radiation. When the potential of the inflaton near the minimum is written as $V \propto \phi^\alpha$, its energy density decreases as $\rho_\phi \propto a^{-6\alpha/(\alpha+2)}$ [32]. Thus the second term can be written as

$$\log \frac{a_{\text{end}}}{a_{\phi\text{reh}}} = \frac{\alpha+2}{6\alpha} \log \frac{\rho_{\phi\text{reh}}}{\rho_{\text{end}}} \simeq \frac{\alpha+2}{3\alpha} \log \frac{\Gamma_\phi}{H_{\text{end}}}, \quad (92)$$

where ρ_{end} and $\rho_{\phi\text{reh}}$ are energy density of inflaton when inflation ends and that of radiation at reheating. For the second approximate equality, we use the sudden decay approximation for the reheating $\Gamma_\phi = H(t_{\phi\text{reh}})$ with Γ_ϕ being the decay rate of the inflaton. For the analysis in the subsequent section, we assume $\Gamma_\phi = 10^{-2}H_{\text{end}}$ for definiteness.

The third term corresponds to $-N_R$ in Eq. (24). The effect of the curvaton on the total e -folding number is contained in this term (see Eq. (31)).

As for the fourth term, we assume that no more entropy is produced after the curvaton decays. Thus this term can be rewritten by using the conservation of the entropy density per comoving volume. Since the entropy density is given by $s = (2\pi/45)g_{*s}T^3$ with g_{*s} being the total number of effective massless degrees of freedom, we have the following relation,

$$\log \frac{a_f}{a_0} = \frac{1}{3} \log \frac{s_0}{s_f} = \frac{1}{3} \log \frac{g_{*s0}T_0^3}{g_{*sf}T_f^3}. \quad (93)$$

For g_{*sf} at the time of a_f , we take $g_{*sf} = 100$.

3 Observational quantities in the mixed models with the inflaton and the curvaton

Now we discuss primordial curvature fluctuations and non-Gaussianity in the mixed models with the inflaton and the curvaton adopting some concrete inflation models. Once

the potential for the inflaton is specified, using the formalism developed above, we can make firm predictions for the scalar spectral index, the tensor-to-scalar ratio and the non-Gaussianity for the model. The issues of the modification to the spectral index, its running and tensor modes have been studied in the case where the energy density of the curvaton should dominate the universe at late time [14, 15, 16]. Here we also include the case where the curvaton is always subdominant in the whole history of the universe. Furthermore, we give the predictions for the non-linearity parameters f_{NL} , τ_{NL} and g_{NL} for inflation models in the scenario. In the following we consider chaotic inflation, new inflation, and hybrid inflation in order.

3.1 Chaotic inflation

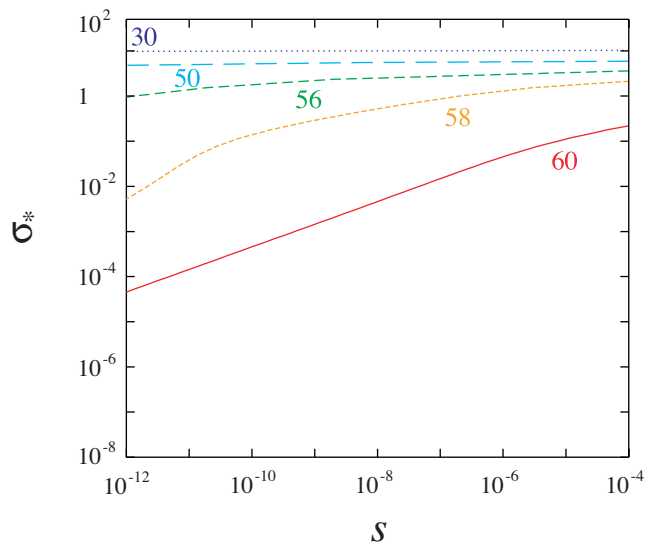


Figure 2: Contours of the e -folding number N in the s - σ_* plane. Here we assumed the chaotic inflation model with $n = 4$ for concreteness. σ_* is shown in units of M_{pl} .

Chaotic inflation [33] is described by the potential of the form,^{#5}

$$V = \lambda M_{\text{pl}}^4 \left(\frac{\phi}{M_{\text{pl}}} \right)^n, \quad (94)$$

where λ is a model parameter which can be fixed by requiring that the fluctuations have the right amplitude to be consistent with observations. To fix the model parameters, we impose the WMAP normalization [42] for the primordial curvature fluctuations given in Eq. (38) to fix the value of λ . For different models of inflation discussed in the following, we also use the WMAP normalization to fix one of the parameters in the inflaton potential.

^{#5}This type of a simple polynomial potential can be realized in supergravity [34, 35, 36, 37, 38, 39, 40, 41].

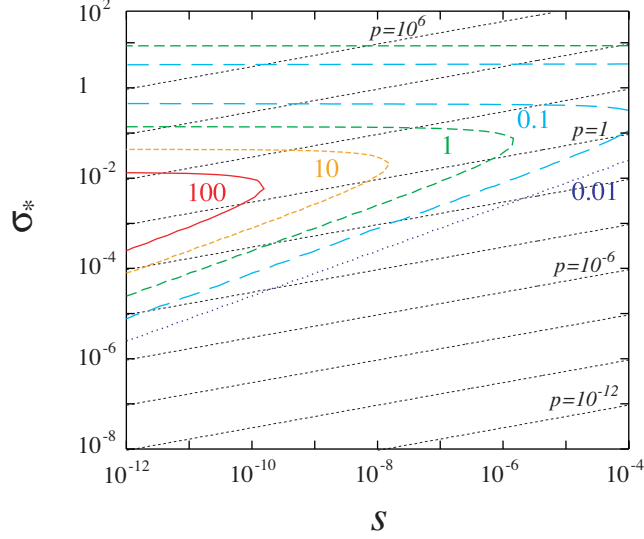


Figure 3: Contours of the ratio of the contribution from the curvaton fluctuation and the inflaton fluctuation $\zeta_{\text{cur}}^2/\zeta_{\text{inf}}^2$ are shown in the s - σ_* plane. Here we assumed the chaotic inflation model with $n = 4$ for concreteness. For reference, we also show contours of p which enables us to see the region where an analytic expression is valid provided in the previous section.

Here we consider some versions of chaotic inflation by taking several values of n which is assumed to be positive even number. With the potential Eq. (94), the slow-roll parameters in this model are given by

$$\epsilon = \frac{1}{2}n^2 \left(\frac{M_{\text{pl}}}{\phi_*} \right)^2, \quad \eta = n(n-1) \left(\frac{M_{\text{pl}}}{\phi_*} \right)^2, \quad \xi^2 = n(n-1)(n-2) \left(\frac{M_{\text{pl}}}{\phi_*} \right)^4. \quad (95)$$

The number of e -folding during inflation can be written as

$$N_{\text{inf}} = \frac{1}{2nM_{\text{pl}}^2}(\phi_*^2 - \phi_{\text{end}})^2, \quad (96)$$

where ϕ_{end} refers to the value of the inflaton at the end of inflation. In general, we can assume $\phi_* \gg \phi_{\text{end}}$. Thus we have a simple relation between ϕ_* and N_{inf} . When fluctuations of the inflaton alone are assumed to exist, the spectral index, its running and the tensor-to-scalar ratio are given by, using the number of e -folding N_{inf} ,

$$n_s - 1 = -\frac{n+2}{2N_{\text{inf}}}, \quad (97)$$

$$n_{\text{run}} = -\frac{n+2}{2N_{\text{inf}}^2}, \quad (98)$$

$$r = \frac{4n}{N_{\text{inf}}}. \quad (99)$$

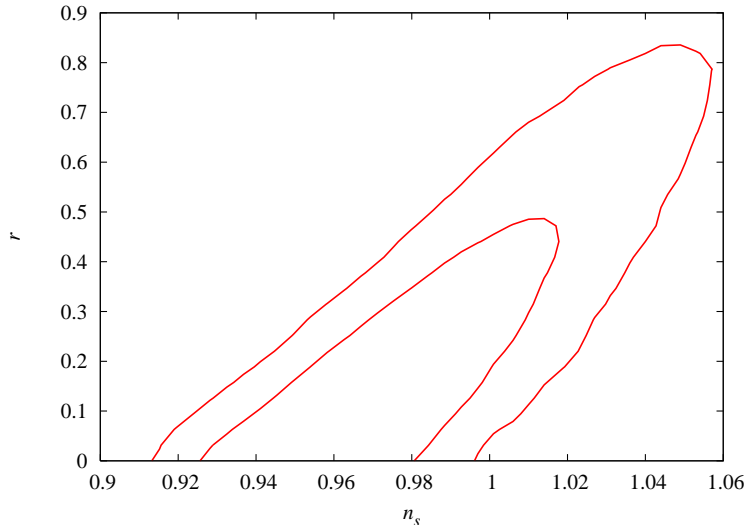


Figure 4: 1σ and 2σ allowed contours from WMAP3 alone are shown, which is generated from the chain provided in the webpage [43].

When fluctuations from the inflaton alone are considered, the non-linearity parameters are very small, which are of the order of slow-roll parameters. An explicit expression can be obtained by setting the curvaton contributions such as Q_σ and $Q_{\sigma\sigma}$ to zero in Eqs. (48), (49) and (50).

In the following, we consider the case with $n = 2, 4$ and 6 , then discuss how the curvaton fluctuations change the predictions of the original inflation models. As we discussed in the previous section, the contribution from the curvaton fluctuations modifies n_s, n_{run} and r as Eqs. (39), (40) and (43). In addition, the curvaton affects the background evolution, which changes the number of e -folding during inflation. When the oscillating curvaton field dominates, its energy density decreases as $\rho_\sigma \propto a^{-3}$. If this phase lasts long, it reduces N_{inf} . When the curvaton drives the second inflation, the number of e -folding is drastically reduced as $N_{\text{inf}} \sim 20\text{--}30$. In this case, as can be read off from Eqs. (97), (98) and (99), the spectral index becomes more red-tilted, its running becomes larger and the tensor-to-scalar ratio is also a bit larger due to the change of N_{inf} . Thus when one considers the effects of the curvaton, the modification to the background evolution is also important.

To see how the curvaton parameters affect the e -folding number during inflation, contours of N_{inf} in the s - σ_* plane are shown in Fig. 2^{#6}. For concreteness, we assumed $n = 4$

^{#6} For the range of s , we take $10^{-12} \leq s \leq 10^{-4}$ in the analysis here. Although s is determined by the combination of the decay rate the curvaton mass as $s = \Gamma_\sigma/m_\sigma$, to make our analysis general, we do not specify the values of Γ_σ and m_σ . However, one should keep in mind that there are some constraints on Γ_σ coming from the bounds on the reheating temperature T_{reh} . A possible upper bound for T_{reh} comes from the consideration of the gravitino problem. To avoid the overproduction of gravitinos, the reheating temperature should be low enough as $T_{\text{reh}} \sim 10^6$ GeV [44, 45]. In addition, $T_{\text{reh}} \sim 10$ MeV is a

to plot the figure. In the figure, σ_* is shown in units of M_{pl} .

As is clearly seen from the figure, when the initial amplitude is large, N_{inf} is significantly reduced due to the second inflation driven by the curvaton. On the other hand, when $\sigma_* \ll M_{\text{pl}}$, dependence of N_{inf} on σ_* and s becomes mild. The qualitative behavior of this result can be understood as follows. There are two possible sources that affect N_{inf} due to the existence of the curvaton. The first one is that the curvaton adds extra e -folding number Q compared to when the curvaton is absent. As a result, N_{inf} must be replaced with $N_{\text{inf}} - Q$. The second one is that if the curvaton fluctuations contribute to the density fluctuations, the energy scale of inflation must decrease so that the sum of the fluctuations originating from both the inflaton and the curvaton satisfies the WMAP normalization. This effect is described by Q_σ . Hence N_{inf} is a function of Q and Q_σ , i.e., $N_{\text{inf}} = N_{\text{inf}}(Q, Q_\sigma)$.

When $\sigma_* \gg M_{\text{pl}}$, Q depends only on σ_* (see Eq. (84)). Hence the slope of the contour in Fig. 2 becomes zero. On the other hand, when $\sigma_* \ll M_{\text{pl}}$, Q becomes a function of p while Q_σ becomes a function of p and σ_*/\sqrt{s} . Hence we can write N_{inf} as $N_{\text{inf}} = N_{\text{inf}}(p, \sigma_*/\sqrt{s})$. When $p \ll 1$, the modification of N_{inf} due to the existence of the curvaton mainly comes from Q_σ which is a function of σ_*/\sqrt{s} at the leading order in p because Q is very small ($Q = \mathcal{O}(p)$). Hence for $p \ll 1$, the slope of the contour approaches $1/4$. When $p \gg 1$, both Q and Q_σ can be important and the slope can vary along the contour.

Furthermore, to see in what range of s and σ_* fluctuations from the curvaton dominates over that from the inflaton, the contours of the ratio of the squared contributions from the curvaton and the inflaton, $\zeta_{\text{cur}}^2/\zeta_{\text{inf}}^2 = 2M_{\text{pl}}^2\epsilon Q_\sigma^2$, are shown in the s - σ_* plane in Fig. 3. For concreteness, we again assumed the chaotic inflation model with $n = 4$. We also plotted contours of $p = \sigma_*^2/(M_{\text{pl}}^2\sqrt{s})$, which enable us to see in what region the analytic estimate we discussed in the previous section can be valid.

Now we discuss the inflationary parameters such as n_s, r and the non-linearity parameters in each case. First we study the case with $n = 2$. In this case, if we assume $N_{\text{inf}} = 50$ and 60, the spectral index and the tensor-to-scalar ratio become $(n_s, r) = (0.96, 0.16)$ and $(n_s, r) = (0.97, 0.13)$, respectively. The running of the spectral index is negligible for this model. To compare these values with observations, we show 1 and 2σ allowed regions from WMAP3 alone analysis in the n_s - r plane in Fig. 4. By looking at the figure, we can see that the case with $n = 2$ is favored by WMAP3 data regardless of the curvaton contribution.

If we include the curvaton, then the non-linearity parameters will become large and n_s and r will also change ^{#7}. Hence it is interesting to check that the inclusion of the curvaton does not spoil the successful values of n_s and r , keeping the non-linearity parameters large.

In Fig. 5, contours of n_s and r are shown for the case with $n = 2$ when the curvaton is included in the s - σ_* plane. With our assumptions explained in the previous section,

possible lower bound not to spoil the success of BBN. (Detailed discussion on this issue can be found in [46, 47, 48, 49, 50].)

^{#7} Even when fluctuation of the curvaton is large enough to affect the values of these quantities, the running of the spectral index remains negligible in this model.

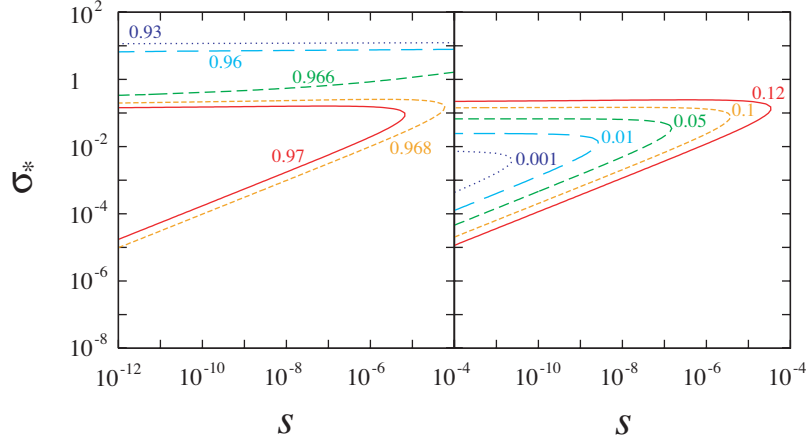


Figure 5: Contours of n_s (left panel) and r (right panel) in the s - σ_* plane for the chaotic inflation model with $n = 2$. In the absence of the curvaton contribution, the spectral index and the tensor-to-scalar ratio are $n_s = 0.967$ and $r = 0.133$ for $N_{\text{inf}} = 60.3$.

the number of e -folding becomes as $N_{\text{inf}} = 60.3$, which yields the spectral index and the tensor-to-scalar ratio as $(n_s, r) = (0.967, 0.133)$ without the curvaton contribution. We can see that, even when the curvaton is introduced to affect the primordial fluctuation, it is consistent with current observations. In Fig. 6, the non-linearity parameters are shown also in the s - σ_* plane. When the curvaton drives the second inflation, the sign of f_{NL} becomes negative and its size is $\mathcal{O}(1)$ in the magnitude. When the curvaton dominates at least once in the history of the universe but there is no second inflation which corresponds to the region where σ_* is small and s is large, the non-linearity parameters become positive but the size is also $\mathcal{O}(1)$. As discussed in the previous section, non-Gaussianity becomes large when $p \ll 1$, which can be seen from the figure. This is why the long axis of contour ellipses lies along the line with $p = \sigma_*^2/M_{\text{pl}}^2\sqrt{s}$ being constant. From the analysis here, it can be concluded that non-Gaussianity can be large when the curvaton also contributes to the primordial fluctuations without spoiling successful values of n_s and r .

Next we discuss the case with $n = 4$. In fact, this model is on the verge of the exclusion even by the WMAP3 data alone. If we assume $N_{\text{inf}} = 60$, the inflationary parameters become $(n_s, r) = (0.95, 0.27)$, which are marginal at the current data. However, by introducing the curvaton in the model, the spectral index is modified to be shifted to the scale-invariant one and the tensor-to-scalar ratio is suppressed. Thus it can liberate the model. In Fig. 7, contours of n_s and r are shown in the s - σ_* plane. Here, in our setting, $N_{\text{inf}} = 60.3$, which yields $(n_s, r) = (0.950, 0.265)$ without the curvaton contribution. When the effects of the curvaton are small, the values of n_s and r fall outside the allowed region. However, in particular, around the region where $\sigma_* \ll M_{\text{pl}}$ and $p \ll 1$, the effects of the curvaton are significant to make the inflationary parameters preferable values in some parameter space. To show in what cases the inflation model is liberated by the curvaton,

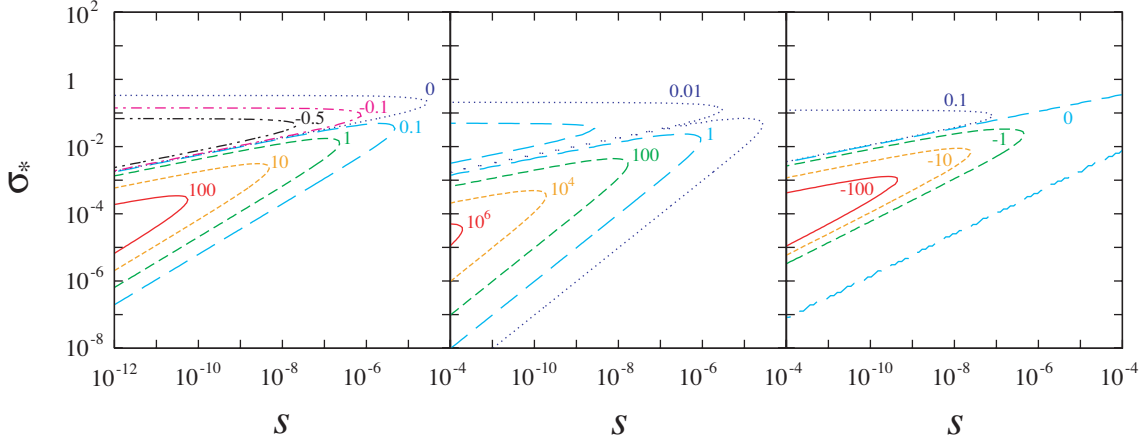


Figure 6: Contours of f_{NL} (left panel), τ_{NL} (center panel) and g_{NL} (right panel) in the s - σ_* plane for the chaotic inflation model with $n = 2$.

the excluded region from the WMAP3 data is represented by the shaded region in Fig. 8. Namely, the region without the shade is allowed by the data. In the same figure, we also plot contours of the non-linearity parameters f_{NL} , τ_{NL} and g_{NL} . Interestingly, there is a parameter space where the model can avoid the exclusion by the data while generating large non-Gaussianity.

As for the case with $n = 6$, this model is completely ruled out by current observations without the curvaton. When $N_{\text{inf}} = 60$ and 50 , the spectral index and the tensor-to-scalar ratio are $(n_s, r) = (0.93, 0.4)$ and $(0.92, 0.48)$. However, in the same way as the case with $n = 4$, this model can be made to be allowed with the help of the curvaton. In Fig. 9, contours of n_s and r are shown. In our setting, $N_{\text{inf}} = 64.0$, which yields $(n_s, r) = (0.937, 0.375)$ without the curvaton contribution. In Fig. 10, contours of the non-linearity parameters are shown along with the region excluded by the data in the s - σ_* plane. Since the original model of inflation is strongly disfavored by the data, the allowed region in Fig. 10 is smaller compared to the counterpart for the case with $n = 4$. However, there is a region where the model is relaxed to be allowed by observations and large non-Gaussianity can be generated.

3.2 New inflation

Among various possibilities of the potential for the new inflation model, we adopt the following form, which is motivated by the supersymmetric models with the discrete R symmetry of the Z_n group [51, 52], for definiteness:

$$V = \lambda^2 v^4 \left[1 - 2 \left(\frac{\phi}{v} \right)^n + \left(\frac{\phi}{v} \right)^{2n} \right]. \quad (100)$$

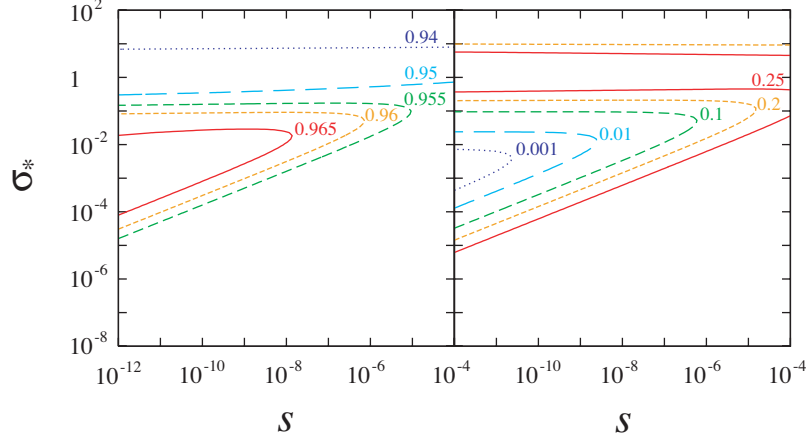


Figure 7: Contours of n_s (left panel) and r (right panel) in the s - σ_* plane for the chaotic inflation model with $n = 4$. In the absence of the curvaton contribution, $n_s = 0.950$ and $r = 0.265$ for $N_{\text{inf}} = 60.3$.

During inflation, the last term in the RHS is irrelevant, thus neglecting this term, we can write down the slow-roll parameters for the potential above as

$$\epsilon = 2n^2 \left(\frac{\phi_*}{v} \right)^{2(n-1)} \left(\frac{M_{\text{pl}}}{v} \right)^2, \quad (101)$$

$$\eta = -2n(n-1) \left(\frac{\phi_*}{v} \right)^{n-2} \left(\frac{M_{\text{pl}}}{v} \right)^2, \quad (102)$$

$$\xi^2 = 4n^2(n-1)(n-2) \left(\frac{\phi_*}{v} \right)^{2(n-2)} \left(\frac{M_{\text{pl}}}{v} \right)^4. \quad (103)$$

The number of e -folding is given approximately as

$$N_{\text{inf}} = \frac{1}{2n(n-2)} \left(\frac{v}{M_{\text{pl}}} \right)^2 \left(\frac{\phi_*}{v} \right)^{-n+2}. \quad (104)$$

Since $\phi_*/v \ll 1$ during inflation, the slow-roll parameter ϵ is much smaller than η in magnitude, which leads to the spectral index $n_s - 1 \simeq 2\eta$. By using N_{inf} , this can be written as

$$n_s - 1 \simeq -2 \frac{n-1}{n-2} \frac{1}{N_{\text{inf}}}. \quad (105)$$

Furthermore, the running of the spectral index $n_{\text{run}} \simeq -2\xi^2$ becomes

$$n_{\text{run}} \simeq -2 \frac{n-1}{n-2} \frac{1}{N_{\text{inf}}^2}. \quad (106)$$

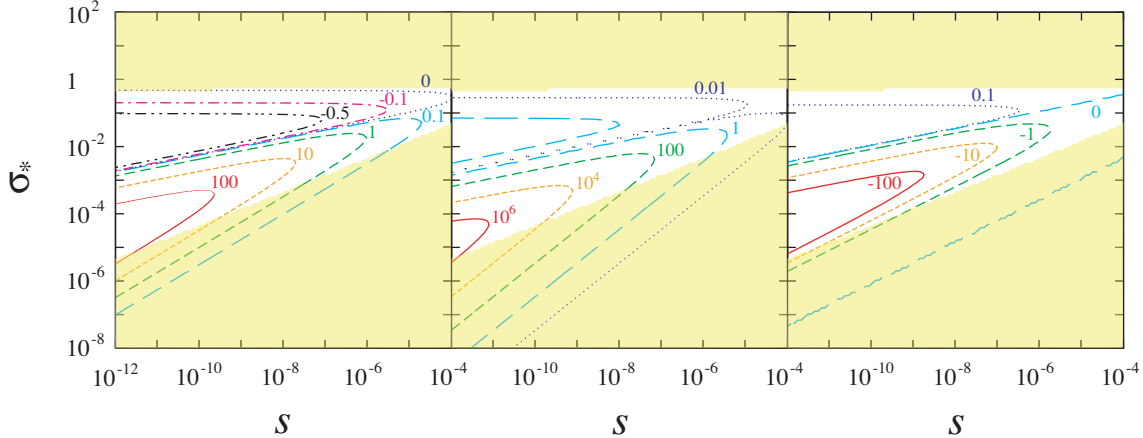


Figure 8: Contours of f_{NL} (left panel), τ_{NL} (center panel) and g_{NL} (right panel) in the s - σ_* plane for the chaotic inflation model with $n = 4$. The shaded region is excluded by WMAP3 data.

The tensor-to-scalar ratio $r = 16\epsilon$ is very small since ϵ is suppressed as

$$\epsilon = 2n^2 \left(\frac{M_{\text{pl}}}{v} \right)^2 \left[\frac{1}{2n(n-2)N_{\text{inf}}} \left(\frac{v}{M_{\text{pl}}} \right) \right]^{2(n-1)/(n-2)}. \quad (107)$$

If we take $n = 3$ and 4 , the ϵ parameters are given by $\epsilon = (v/M_{\text{pl}})^6/(72N_{\text{inf}}^4)$ and $\epsilon = 4(v/M_{\text{pl}})^4/(27N_{\text{inf}}^3)$, respectively. Thus even if we take $v \sim M_{\text{pl}}$, ϵ is suppressed with some powers of N_{inf} which is usually 50–60. Hence both the tensor-to-scalar ratio and the running are very small in this model. The spectral indices for the cases with $n = 3$ and 4 are $n_s = 0.93$ and 0.95 when $N_{\text{inf}} = 60$. Thus this model is almost consistent with the current constraint from WMAP3 in terms of the spectral index and tensor mode.

One may speculate that, adding a contribution from the curvaton, non-Gaussianity becomes significantly large like in the case of the chaotic inflation. However, this does not happen in the new inflation. This is because the slow-roll parameter ϵ is very small in the new inflation models. Largest possible values for the non-linear parameters which are given in Eqs. (72), (73) and (74) indicate that these values are proportional to ϵ . Thus inflation models with small ϵ cannot generate large non-Gaussianity even by adding the curvaton.

Furthermore, when ϵ is very small, the effects of the curvaton on n_s and r are also small. As seen from Eqs. (39), (40) and (43), the effect of the curvaton on these quantities always appears in the combination of ϵQ_σ^2 . Thus even when Q_σ is large, this combination is small if ϵ is negligibly small. To see this fact, contours of n_s for the case with $n = 3$ and 4 are shown in Fig. 11. In both case, we take $v = 10^{-2}M_{\text{pl}}$. Without the curvaton contribution, the e -folding numbers in our setting for $n = 3$ and 4 are given by $N_{\text{inf}} = 50.3$ and 53.3 respectively. Then the spectral indices are $n_s = 0.920$ and 0.944 respectively. As seen from the figure, the value of n_s does not change much over the whole parameter space

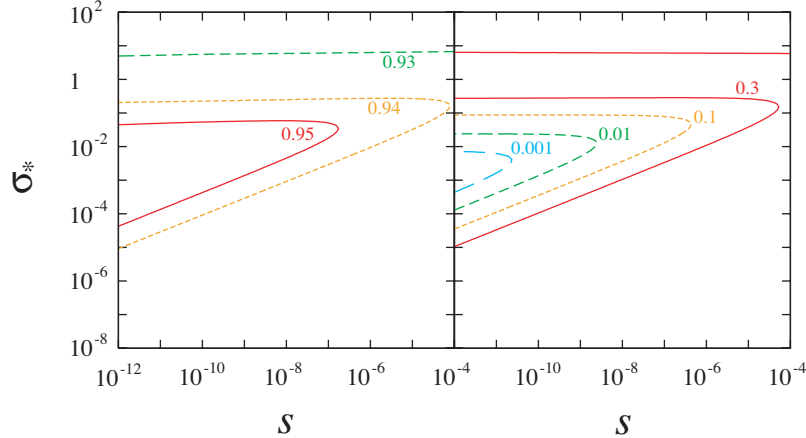


Figure 9: Contours of n_s (left panel) and r (right panel) in the s - σ_* plane for the chaotic inflation model with $n = 6$. In the absence of the curvaton contribution, the spectral index and the tensor-to-scalar ratio are $n_s = 0.937$ and $r = 0.375$ for $N_{\text{inf}} = 64.0$.

in the figure. This indicates that the effect of the curvaton cannot be large for a broad range of the curvaton parameters. In fact, when the initial amplitude for the curvaton is large, n_s is modified a little because of the change of the number of e -folding due to the second inflation. However, in any case, the figure clearly shows that the effect of the fluctuations of the curvaton is small for this kind of models.

3.3 Hybrid inflation

Hybrid inflation was originally proposed by Linde [53, 54] and many types of the potential have been discussed in association with the gauge symmetry breaking [55, 56, 57]. Here, we take the original types of the potential for simplicity. The implications of another field on other types of the potential like those in the supersymmetric grand unified theory are discussed in the context of modular inflation [58].

We consider the following quadratic type of potential,

$$V = \alpha \left[(v^2 - \sigma^2)^2 + \frac{m^2}{2} \phi^2 + \frac{g^2}{2} \phi^2 \sigma^2 \right]. \quad (108)$$

Here we set the parameters to be $v = 10^{-2} M_{\text{pl}}$, $m = 2 \times 10^{-5} M_{\text{pl}}$, and $g = 2 \times 10^{-3}$. The parameter α is chosen to fit the WMAP normalization. For $\phi > \phi_{\text{end}} = 2v/g = 10 M_{\text{pl}}$, the trajectory with $\sigma = 0$ is stable and inflation takes place along this trajectory with the effective potential given by $V_{\text{eff}}(\phi) = \alpha(v^4 + m^2 \phi^2/2)$. Then, the slow-roll parameters are given by

$$\epsilon = \frac{1}{2} \left(\frac{m^2 M_{\text{pl}} \phi}{v^4 + \frac{1}{2} m^2 \phi^2} \right)^2, \quad \eta = \frac{m^2 M_{\text{pl}}^2}{v^4 + \frac{1}{2} m^2 \phi^2}, \quad \xi^2 = 0. \quad (109)$$

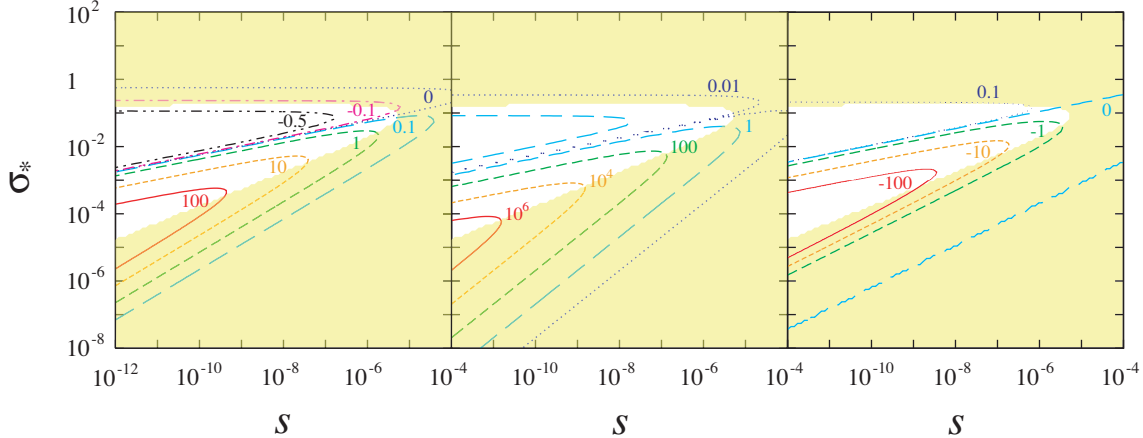


Figure 10: Contours of f_{NL} (left panel), τ_{NL} (center panel) and g_{NL} (right panel) in the s - σ_* plane for the chaotic inflation model with $n = 6$. The shaded region is excluded by WMAP3 data.

For the parameters above, without the curvaton contribution, the number of e -folding, the spectral index and the tensor-to-scalar ratio are given by $N_{\text{inf}} = 55.3$, $n_s = 0.975$ and $r = 0.118$. The running of the spectral index is negligible in this case. Although these values are consistent with the WMAP3 data, to see how the curvaton affects these predictions, contours of n_s and r are shown in Fig. 12. Furthermore, contours of non-linearity parameters are also shown in Fig. 13. In this case, large non-Gaussianity can also be generated.

In the above choice of the parameters, we have red-tilted power spectrum in the absence of the curvaton. We can choose another set of parameters such that $m \ll gv$. In this case, we have $\eta \gg \epsilon$ and the spectrum becomes blue, i.e., $n_s \approx 1 + 6\eta$, in the absence of the curvaton. If the curvaton contribution is small enough to satisfy $\epsilon M_{\text{pl}}^2 Q_\sigma^2 \ll 1$, then adding the curvaton yields no effects on the parameters as in the case of the new inflation. On the other hand, if the curvaton contribution is large enough to satisfy $\epsilon M_{\text{pl}}^2 Q_\sigma^2 \gg 1$, then the spectral index is given by $n_s - 1 \approx -2\epsilon + \eta/(\epsilon M_{\text{pl}}^2 Q_\sigma^2)$. Because ϵ is very small ($\epsilon \ll \eta$) and η is positive in this model, the spectrum is almost scale invariant or blue-tilted, and r is negligibly small. Hence, for $m \ll gv$ in which case the spectrum is blue with negligibly small scalar-to-tensor ratio, the model with such parameters is hardly allowed by WMAP3 (see Fig. 4) even if the curvaton contributes to the primordial fluctuations.

4 Summary and Discussions

In this paper, we studied primordial fluctuations in models where both the inflaton and the curvaton can contribute to the cosmic density fluctuations. By using the δN formalism, we provided a systematic formulation to discuss the primordial curvature fluctuations and

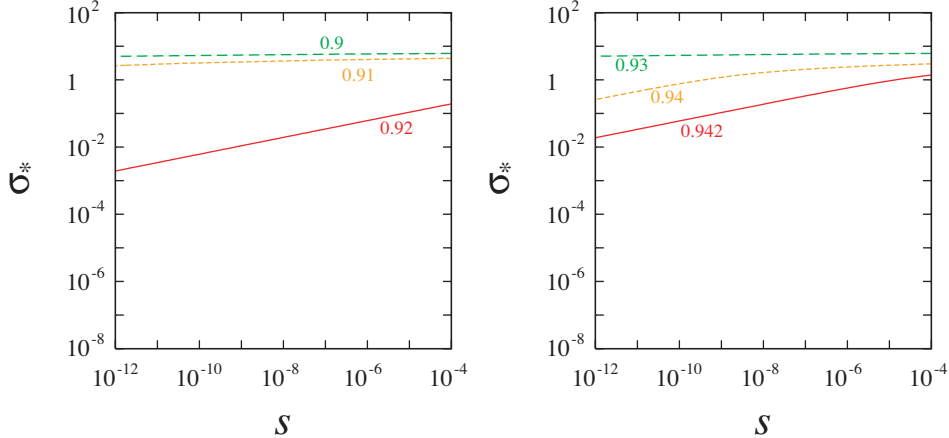


Figure 11: Contours of n_s in the s - σ_* plane for the new inflation model with $n = 3$ (left) and $n = 4$ (right). We take $v = 10^{-2}M_{\text{pl}}$. In the absence of the curvaton contribution, $n_s = 0.920$ and 0.944 for the case with $n = 3, N_{\text{inf}} = 50.3$ and $n = 4, N_{\text{inf}} = 53.3$ respectively.

their non-Gaussianity in this kind of scenario. We gave the expressions for the spectral index n_s , its running n_{run} , the tensor-to-scalar ratio r and the non-linearity parameters $f_{\text{NL}}, \tau_{\text{NL}}$ and g_{NL} for the mixed model. In general, the values of these parameters can be obtained by numerically calculating some set of equations, however, in some cases, they are given analytically. We presented such analytic formulae in some limiting cases. We found that very large non-Gaussianity ($f_{\text{NL}} \gg 1$) can be generated even if the contribution of the curvaton fluctuations to the total ones is comparable to or smaller than that of the inflaton fluctuations. If the curvaton fluctuations are minor components, then τ_{NL} is enhanced by the factor of $\zeta_{\text{inf}}^2/\zeta_{\text{cur}}^2 \gg 1$, compared to f_{NL}^2 , where ζ_{inf} and ζ_{cur} are the primordial fluctuations from the inflaton and the curvaton respectively. In such a case, large non-Gaussian feature appears through the trispectrum rather than through the bispectrum. We also derived the consistency relation between the bispectrum and the trispectrum which holds in the limit of the large non-Gaussianity. If the measurement of the trispectrum becomes available in the future, this relation will provide a useful tool to distinguish the mixed model of the inflaton and the curvaton from other scenarios which also generate large non-Gaussianity.

After we worked out the formulation for the calculation of inflationary parameters including the non-linearity parameters, we investigated the issue for several concrete models of inflation: chaotic inflation, new inflation and hybrid inflation. By calculating the spectral index and the tensor-to-scalar ratio, we can compare those with cosmological observations. We showed that some inflation models already excluded by the current data such as chaotic inflation with higher polynomials $n = 4$ and 6 can be liberated depending on the parameters which characterize the curvaton. By presenting contours of n_s and r in

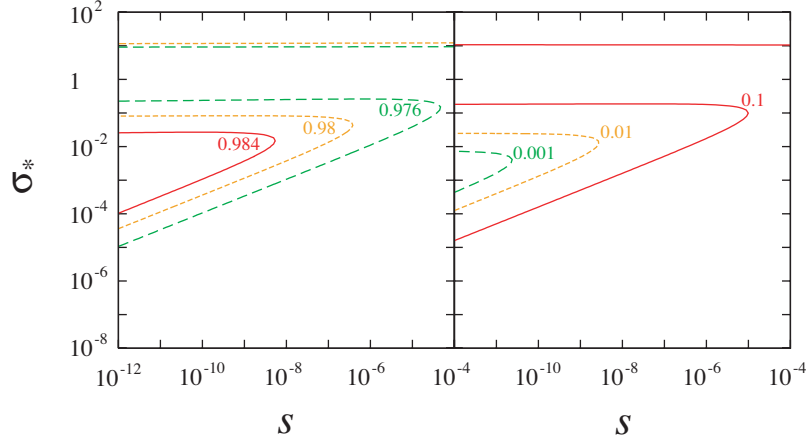


Figure 12: Contours of n_s (left panel) and r (right panel) in the s - σ_* plane for the hybrid inflation model with a quadratic potential. In the absence of the curvaton contribution, the spectral index and tensor-to-scalar ratio become as $n_s = 0.975$ and $r = 0.118$ for $N_{\text{inf}} = 55.3$.

the s - σ_* plane, we have explicitly shown in what cases such models can be relaxed to be allowed by the data. We have also presented contours of the non-linearity parameters in the s - σ_* plane. In particular, it should be noticed that, the non-Gaussianity can be large due to the contribution from the curvaton without conflicting with the data.

On the other hand, some inflation models such as the new inflation where the slow-roll parameter ϵ is very small are scarcely affected by the curvaton. The effects of the curvaton on n_s and r appear as in the combination of ϵQ_σ^2 , thus the size of ϵ is crucial when one considers how the curvaton affects the inflationary predictions. Furthermore, non-Gaussianity cannot be large in this model even if we introduce the curvaton because the ϵ parameter is very small in this model. As shown in Eqs. (48)~(50), the curvaton contribution to the non-linearity parameters is always associated with ϵ . Thus inflation models with very small ϵ cannot generate large non-Gaussianity even with the curvaton.

Although we have concentrated on adiabatic fluctuations thus far, isocurvature fluctuations can be produced in principle, depending on the thermal history of the universe. It can happen when dark matter or baryon was generated (and its number is conserved) before the decay of the curvaton or from the decay products of the curvaton [59, 60, 61]. In the case where dark matter and baryon were produced after the decay of the curvaton, no isocurvature perturbation is generated even in our mixed model. In this paper, we have considered this kind of case to avoid complexities coming from the contamination of isocurvature modes when we interpret observational signatures. However, here we comment on the cases where some isocurvature fluctuations are generated. First of all, since pure cold dark matter (CDM)/baryon isocurvature modes (regardless of its correlation with adiabatic mode) are severely constrained by observations, the pure curvaton scenario

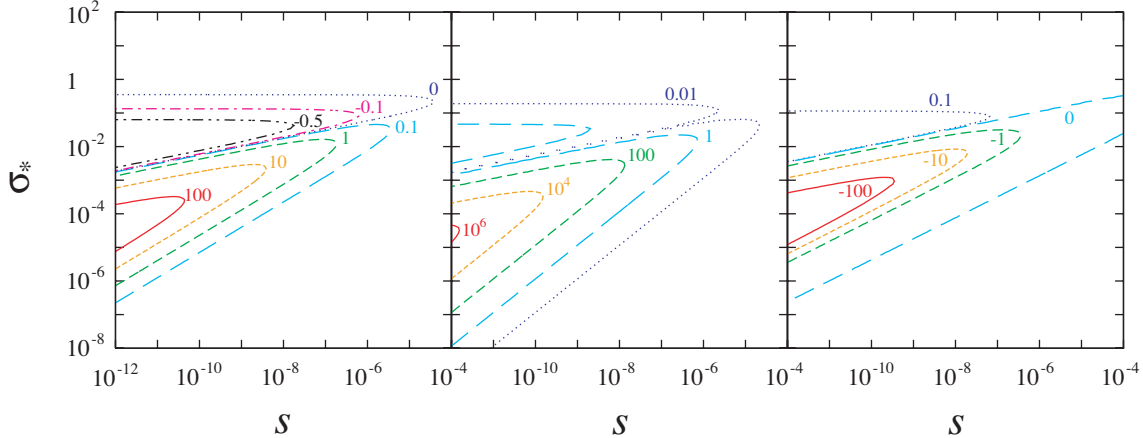


Figure 13: Contours of f_{NL} (left panel), τ_{NL} (center panel) and g_{NL} (right panel) in the s - σ_* plane for the hybrid inflation model with a quadratic potential.

with isocurvature fluctuations such as the above mentioned cases are disfavored from current observations. However, it should be noted here that the constraint can be relaxed when adiabatic fluctuations from the inflaton contribute to the total density fluctuations, which is the case for the mixed scenario. This is simply because the contribution from adiabatic mode decreases the fraction of the isocurvature contribution to the total fluctuations. Thus the mixed scenario may have interesting implications on scenarios with isocurvature fluctuations. For example, even in the case where dark matter was generated before the decay of the curvaton, the mixed scenario is still allowed if adiabatic fluctuations from the inflaton is bigger than that from the curvaton to some extent. Similarly, although a scenario where dark matter was generated from the decay products of the curvaton is severely constrained by the argument of isocurvature fluctuations, as in the case discussed above, the constraint is significantly relaxed in the mixed scenario if adiabatic fluctuation from the inflaton is much bigger than that from the curvaton. It should be noticed that large non-Gaussianity would not be produced when the contribution from the inflaton is large compared to that from the curvaton. On the other hand, when the contribution from the curvaton with isocurvature mode is large, such a scenario is severely constrained by the consideration of isocurvature mode, which corresponds to the case where the fraction of energy density of the curvaton to the total one becomes comparable to that of the inflaton. Remind that large non-Gaussianity can be generated when the fraction of energy density of the curvaton to the total one is very small. Thus non-Gaussianity would not be so large in this case too.

Since a simple single-field inflation model can only generate very small non-Gaussianity, if the evidence of non-Gaussianity, which was recently reported in Ref. [3], is established in the future, this mechanism of generating large non-Gaussianity will be very interesting. Although we concentrate on the mixed model of the inflaton and the curvaton in this paper, other mixed model may also be worth investigating. In particular, large non-Gaussianity

can also be generated in the modulated reheating [62, 63, 64, 27] and preheating scenarios [65, 66, 67] so that the implications of such a mixed model on the inflationary parameters and non-Gaussianity are of great interest and will be presented elsewhere [68].

Acknowledgments: This work is supported in part by the Sumitomo Foundation (T.T.) and the Grant-in-Aid for Scientific Research from the Ministry of Education, Science, Sports, and Culture of Japan No.18840010 (K.I.), No.19740145 (T.T.), No.18740157, and No.19340054 (M.Y.). TS thanks to the computer system at the Yukawa Institute for Theoretical Physics, Kyoto University, for the numerical calculations.

Appendix

A Value of σ at the onset of the curvaton oscillations

In the main text, we defined $g(\sigma_*)$ with the energy density of the curvaton at the onset of the oscillations as

$$\rho_\sigma(N_m) = \frac{1}{2}m_\sigma^2 g(\sigma_*)^2, \quad (110)$$

with $g(\sigma_*) = \alpha\sigma_*$. We assume that the universe is radiation-dominated when the curvaton begins to oscillate, thus the equation of motion for σ can be written as

$$\ddot{\sigma} + \frac{3}{2t}\dot{\sigma} + m_\sigma^2\sigma = 0, \quad (111)$$

where we used $H = 1/(2t)$ during radiation-dominated epoch. The solution for this equation with the initial value $\sigma(t_m) = \sigma_*$ is given by

$$\sigma(t) = \frac{2^{1/4}\Gamma(5/4)\sigma_*}{(mt)^{1/4}}J_{1/4}(mt), \quad (112)$$

where J is the Bessel function. Using the asymptotic form of $J_{1/4}$, the energy density ρ_σ for $mt \gg 1$ becomes

$$\rho_\sigma(t) \simeq \frac{\sqrt{2}m_\sigma^2\sigma_*^2}{\pi(mt)^{3/2}}\Gamma(5/4). \quad (113)$$

Thus α can be given by

$$\alpha = \frac{2\sqrt{2}}{\sqrt{\pi}}\Gamma(5/4) \simeq 1.45. \quad (114)$$

B Analytic expression of $F(p)$ for $p \ll 1$

In this Appendix, we give a detailed description how we obtain an analytic expression of $F(p)$ for the case with $p \ll 1$. We also assume that the value of $s = \Gamma_\sigma/m_\sigma$ is also very small. $F(p)$ is given as

$$F(p) = \int_0^\infty dN e^{4N} \frac{\Gamma_\sigma}{H(N)} \frac{\rho_\sigma(N)}{\rho_{r0}}. \quad (115)$$

To evaluate $F(p)$, we have to follow the evolution of energy densities of the curvaton and radiation after the curvaton begins to oscillate for the case we are going to consider here. Thus we take the initial time $N = 0$ when H is equal to m_σ and the curvaton field can be

considered to be dust. In this case, the background equations we need to follow are:

$$\frac{d}{dN}\rho_r + 4\rho_r = \frac{\Gamma_\sigma}{H}\rho_\sigma, \quad (116)$$

$$\frac{d}{dN}\rho_\sigma + 3\rho_\sigma = -\frac{\Gamma_\sigma}{H}\rho_\sigma, \quad (117)$$

$$H^2 = \frac{1}{3M_{\text{pl}}^2}(\rho_r + \rho_\sigma), \quad (118)$$

where we use the number of e -folding as a time variable. We solve this set of equations with the initial conditions:

$$\rho_r(0) = \rho_{r0}, \quad \rho_\sigma(0) = \rho_{\sigma0} = \frac{\alpha^2 m_\sigma^2 \sigma_*^2}{2}, \quad H(0) = H_0 = m_\sigma. \quad (119)$$

We assume that curvaton energy density is negligibly small throughout the evolution. Hence we treat $\rho_{\sigma0}$ as the expansion parameter of order p , where p is infinitesimal. Then we can expand ρ_r, ρ_σ, H with respect to p as

$$\rho_r = \rho_r^{(0)} + \rho_r^{(1)} + \rho_r^{(2)} + \dots, \quad (120)$$

$$\rho_\sigma = \rho_\sigma^{(0)} + \rho_\sigma^{(1)} + \rho_\sigma^{(2)} + \dots, \quad (121)$$

$$H = H^{(0)} + H^{(1)} + H^{(2)} + \dots, \quad (122)$$

where $\rho_r^{(n)}, \rho_\sigma^{(n)}, H^{(n)} = \mathcal{O}(p^n)$. We also expand $F(p)$ with respect to p as

$$F = F^{(0)} + F^{(1)} + F^{(2)} + \dots. \quad (123)$$

Obviously, $F^{(0)}$ vanishes. We are going to obtain the expression for $F(p)$ by solving the above set of equations order by order in the following.

• 0th order in p

Since the energy density of the curvaton field is considered to be the order of $\mathcal{O}(p)$, at the 0-th order, it vanishes as $\rho_\sigma^{(0)} = 0$. Other quantities can be easily obtained.

$$\rho_r^{(0)} = \rho_{r0}e^{-4N}, \quad H^{(0)} = H_0e^{-2N}. \quad (124)$$

• 1st order in p

From Eq. (117), the equation for $\rho_\sigma^{(1)}$ can be written as

$$\frac{d}{dN}\rho_\sigma^{(1)} + 3\rho_\sigma^{(1)} = -se^{2N}\rho_\sigma^{(1)}. \quad (125)$$

By solving this equation, the energy density of the curvaton in the 1st order is given by

$$\rho_\sigma^{(1)} = \rho_{\sigma0} \exp \left[-3N - \frac{s}{2}(e^{2N} - 1) \right]. \quad (126)$$

At the 1st order in p , $F(p)$ can be given by

$$F^{(1)}(p) = \int_0^\infty dN e^{4N} \frac{\Gamma_\sigma}{H^{(0)}} \frac{\rho_\sigma^{(1)}}{\rho_{r0}}. \quad (127)$$

By substituting the expressions for $\rho_\sigma^{(1)}$ and $H^{(0)}$ into the above equation, we obtain

$$F^{(1)}(p) = \int_0^\infty dN e^{4N} \frac{\Gamma_\sigma}{H_0 e^{-2N}} \frac{\rho_{\sigma 0}}{3H_0^2 M_{\text{pl}}^2} \exp \left[-3N - \frac{\Gamma_\sigma}{2H_0} (e^{2N} - 1) \right]. \quad (128)$$

The integral which appears in this equation can be done analytically as,

$$\int_0^\infty dN \exp \left[3N - \frac{\Gamma_\sigma}{2m_\sigma} (e^{2N} - 1) \right] = \sqrt{\frac{1}{2s^3}} \left(\sqrt{2s} + \sqrt{\pi} e^{s/2} \left(1 - \text{Erf}(\sqrt{s/2}) \right) \right). \quad (129)$$

where $\text{Erf}(x)$ is the error function and defined by

$$\text{Erf}(x) \equiv \frac{2}{\sqrt{\pi}} \int_0^x dt e^{-t^2}. \quad (130)$$

By expanding the error function with s and taking the leading order, we can obtain F at the first order in p as

$$F^{(1)}(p) = \frac{1}{6} \sqrt{\frac{\pi}{2}} \alpha^2 p. \quad (131)$$

To evaluate the function $F(p)$ at the second order, we need the expressions for $\rho_r^{(1)}$ and $H^{(1)}$. For the energy density of radiation for the 1st order, from Eq. (116), we have the equation for $\rho_r^{(1)}$ as

$$\frac{d}{dN} \rho_r^{(1)} + 4\rho_r^{(1)} = s e^{2N} \rho_\sigma^{(1)}. \quad (132)$$

Using Eq. (126), the solution of this equation can be formally written as

$$\rho_r^{(1)} = s \rho_{\sigma 0} e^{-4N} \int_0^N dN' \exp \left(3N' - \frac{s}{2} (e^{2N'} - 1) \right). \quad (133)$$

By plugging this expression into the Friedmann equation, the Hubble parameter can be given by, in the 1st order,

$$\frac{H^{(1)}}{H^{(0)}} = \frac{1}{2} \frac{\rho_{\sigma 0}}{\rho_{r0}} e^{\frac{s}{2}} \left[s \int_0^N dN' \exp \left(3N' - \frac{s}{2} e^{2N'} \right) + \exp \left(N - \frac{s}{2} e^{2N} \right) \right]. \quad (134)$$

• 2nd order in p

Now we calculate the function $F(p)$ for the second order in p . $F^{(2)}(p)$ can be written as

$$F^{(2)} = s \int_0^\infty dN e^{6N} \frac{\rho_\sigma^{(2)}}{\rho_{r0}} - s \int_0^\infty dN e^{6N} \frac{H^{(1)}}{H^{(0)}} \frac{\rho_\sigma^{(1)}}{\rho_{r0}}. \quad (135)$$

To evaluate the RHS, we do not need $\rho_r^{(2)}$ and $H^{(2)}$ because these do not appear in $F(p)$ up to second order in p , but we need to have the expression for $\rho_\sigma^{(2)}$. From Eq. (117), we have an equation for $\rho_\sigma^{(2)}$ as

$$\frac{d}{dN}\rho_\sigma^{(2)} + 3\rho_\sigma^{(2)} = -se^{2N}\rho_\sigma^{(2)} + se^{2N}\frac{H^{(1)}}{H^{(0)}}\rho_\sigma^{(1)}. \quad (136)$$

Using the first order solutions obtained above, $\rho_\sigma^{(2)}$ can be written as

$$\begin{aligned} \rho_\sigma^{(2)} = & \frac{s}{2} \frac{\rho_{\sigma 0}}{\rho_{r 0}} \rho_{\sigma 0} e^s \exp\left(-3N - \frac{s}{2}e^{2N}\right) \int_0^N dN' e^{2N'} \\ & \times \left[s \int_0^{N'} dN'' \exp\left(3N'' - \frac{s}{2}e^{2N''}\right) + \exp\left(N' - \frac{s}{2}e^{2N'}\right) \right]. \end{aligned} \quad (137)$$

In principle, $F^{(2)}$ can be obtained by plugging Eqs. (133), (134) and (137) into Eq. (135), the expression becomes lengthy and complicated, we consider each term in the RHS of Eq. (135) in each.

We denote the first term in Eq. (135) as T_1 . Using the formulae for $\rho_r^{(1)}$ and $H^{(1)}$, T_1 can be written as

$$\begin{aligned} T_1 = & \frac{s^2}{2} \left(\frac{\rho_{\sigma 0}}{\rho_{r 0}} \right)^2 e^s \int_0^\infty dN \exp\left(3N - \frac{s}{2}e^{2N}\right) \int_0^N dN' e^{2N'} \\ & \times \left[s \int_0^{N'} dN'' \exp\left(3N'' - \frac{s}{2}e^{2N''}\right) + \exp\left(N' - \frac{s}{2}e^{2N'}\right) \right]. \end{aligned} \quad (138)$$

Although we need to perform a triple integral, we can make use the following formula^{#8}:

$$\int_0^N dN' \exp\left(3N' - \frac{s}{2}e^{2N'}\right) \simeq \left(\frac{2}{s}\right)^{3/2} \left[-\frac{1}{2}\sqrt{\frac{s}{2}} \exp\left(N - \frac{s}{2}e^{2N}\right) + \frac{\sqrt{\pi}}{4} \text{Erf}\left(\sqrt{\frac{s}{2}}e^N\right) \right], \quad (140)$$

where we have neglected higher order terms in s because we are interested in the case $s \ll 1$. Using this formula, the first term in Eq. (138) can be written as β_1/s^3 (omitting the factor appearing outside the integral and taking only leading order term in s) where β_1 is given by

$$\beta_1 \equiv 8 \int_0^\infty dy y^2 e^{-y^2} \int_0^y dx \left(-x^2 e^{-x^2} + \frac{\sqrt{\pi}}{2} x \text{Erf}(x) \right). \quad (141)$$

^{#8} This equation can be verified by changing the variable as

$$\sqrt{\frac{s}{2}}e^N = y. \quad (139)$$

After some calculations, we find $\beta_1 = 1$. The second term in Eq. (138) can be calculated as $\pi/(4s^3)$. Hence T_1 is given by

$$T_1 = \frac{1}{2s} \left(\frac{\rho_{\sigma 0}}{\rho_{r 0}} \right)^2 \left(1 + \frac{\pi}{4} \right). \quad (142)$$

Next we evaluate the second term in Eq. (135) which is denoted as T_2 . By using the expressions for $\rho_{\sigma}^{(1)}$ and $H^{(1)}$, T_2 can be written as

$$T_2 = \frac{s}{2} \left(\frac{\rho_{\sigma 0}}{\rho_{r 0}} \right)^2 e^s \int_0^{\infty} dN \exp \left(3N - \frac{s}{2} e^{2N} \right) \times \left[s \int_0^N dN' \exp \left(3N' - \frac{s}{2} e^{2N'} \right) + \exp \left(N - \frac{s}{2} e^{2N} \right) \right]. \quad (143)$$

Similar calculations to the case with T_1 yields

$$T_2 = \frac{1}{4s} \left(1 + \frac{\pi}{2} \right) \left(\frac{\rho_{\sigma 0}}{\rho_{r 0}} \right)^2, \quad (144)$$

where we have again dropped higher order terms in s . Thus we obtain the expression for $F^{(2)}$ as

$$F^{(2)} = T_1 - T_2 = \frac{\alpha^4}{144} p^2. \quad (145)$$

References

- [1] D. N. Spergel *et al.* [WMAP Collaboration], *Astrophys. J. Suppl.* **170**, 377 (2007) [arXiv:astro-ph/0603449].
- [2] M. Tegmark *et al.* [SDSS Collaboration], *Phys. Rev. D* **74**, 123507 (2006) [arXiv:astro-ph/0608632].
- [3] A. P. S. Yadav and B. D. Wandelt, arXiv:0712.1148 [astro-ph].
- [4] K. Enqvist and M. S. Sloth, *Nucl. Phys. B* **626**, 395 (2002) [arXiv:hep-ph/0109214];
- [5] D. H. Lyth and D. Wands, *Phys. Lett. B* **524**, 5 (2002) [arXiv:hep-ph/0110002];
- [6] T. Moroi and T. Takahashi, *Phys. Lett. B* **522**, 215 (2001) [Erratum-ibid. B **539**, 303 (2002)] [arXiv:hep-ph/0110096].
- [7] G. Dvali, A. Gruzinov and M. Zaldarriaga, *Phys. Rev. D* **69**, 023505 (2004) [arXiv:astro-ph/0303591].

- [8] L. Kofman, arXiv:astro-ph/0303614.
- [9] K. Dimopoulos and D. H. Lyth, Phys. Rev. D **69**, 123509 (2004) [arXiv:hep-ph/0209180].
- [10] M. Endo, M. Kawasaki and T. Moroi, Phys. Lett. B **569**, 73 (2003) [arXiv:hep-ph/0304126].
- [11] G. Lazarides, R. R. de Austri and R. Trotta, Phys. Rev. D **70**, 123527 (2004) [arXiv:hep-ph/0409335].
- [12] K. Dimopoulos, D. H. Lyth and Y. Rodriguez, JHEP **0502**, 055 (2005) [arXiv:hep-ph/0411119].
- [13] Y. Rodriguez, Mod. Phys. Lett. A **20**, 2057 (2005) [arXiv:hep-ph/0411120].
- [14] D. Langlois and F. Vernizzi, Phys. Rev. D **70**, 063522 (2004) [arXiv:astro-ph/0403258].
- [15] T. Moroi, T. Takahashi and Y. Toyoda, Phys. Rev. D **72**, 023502 (2005) [arXiv:hep-ph/0501007].
- [16] T. Moroi and T. Takahashi, Phys. Rev. D **72**, 023505 (2005) [arXiv:astro-ph/0505339].
- [17] A. A. Starobinsky, JETP Lett. **42** (1985) 152 [Pisma Zh. Eksp. Teor. Fiz. **42** (1985) 124].
- [18] M. Sasaki and E. D. Stewart, Prog. Theor. Phys. **95**, 71 (1996) [arXiv:astro-ph/9507001].
- [19] M. Sasaki and T. Tanaka, Prog. Theor. Phys. **99**, 763 (1998) [arXiv:gr-qc/9801017].
- [20] D. H. Lyth, K. A. Malik and M. Sasaki, JCAP **0505**, 004 (2005) [arXiv:astro-ph/0411220].
- [21] D. Seery and J. E. Lidsey, JCAP **0509**, 011 (2005) [arXiv:astro-ph/0506056].
- [22] D. Seery, J. E. Lidsey and M. S. Sloth, JCAP **0701**, 027 (2007) [arXiv:astro-ph/0610210].
- [23] F. Arroja and K. Koyama, arXiv:0802.1167 [hep-th].
- [24] D. H. Lyth and Y. Rodriguez, Phys. Rev. Lett. **95**, 121302 (2005) [arXiv:astro-ph/0504045].
- [25] L. Alabidi and D. H. Lyth, JCAP **0605**, 016 (2006) [arXiv:astro-ph/0510441].

- [26] C. T. Byrnes, M. Sasaki and D. Wands, Phys. Rev. D **74**, 123519 (2006) [arXiv:astro-ph/0611075].
- [27] T. Suyama and M. Yamaguchi, Phys. Rev. D **77**, 023505 (2008) [arXiv:0709.2545 [astro-ph]].
- [28] D. Polarski and A. A. Starobinsky, Nucl. Phys. B **385**, 623 (1992).
- [29] K. A. Malik, D. Wands and C. Ungarelli, Phys. Rev. D **67**, 063516 (2003) [arXiv:astro-ph/0211602].
- [30] S. Gupta, K. A. Malik and D. Wands, Phys. Rev. D **69**, 063513 (2004) [arXiv:astro-ph/0311562].
- [31] Q. G. Huang, arXiv:0801.0467 [hep-th].
- [32] M. S. Turner, Phys. Rev. D **28**, 1243 (1983).
- [33] A. D. Linde, Phys. Lett. B **129**, 177 (1983).
- [34] A. B. Goncharov and A. D. Linde, Phys. Lett. B **139**, 27 (1984).
- [35] A. S. Goncharov and A. D. Linde, Class. Quant. Grav. **1**, L75 (1984).
- [36] H. Murayama, H. Suzuki, T. Yanagida and J. Yokoyama, Phys. Rev. D **50**, 2356 (1994) [arXiv:hep-ph/9311326].
- [37] M. Kawasaki, M. Yamaguchi and T. Yanagida, Phys. Rev. Lett. **85**, 3572 (2000) [arXiv:hep-ph/0004243].
- [38] M. Kawasaki, M. Yamaguchi and T. Yanagida, Phys. Rev. D **63**, 103514 (2001) [arXiv:hep-ph/0011104].
- [39] K. Kadota and M. Yamaguchi, Phys. Rev. D **76**, 103522 (2007) [arXiv:0706.2676 [hep-ph]].
- [40] T. Kawano, arXiv:0712.2351 [hep-th].
- [41] K. Kadota, T. Kawano and M. Yamaguchi, arXiv:0802.0525 [hep-ph].
- [42] A. R. Liddle, D. Parkinson, S. M. Leach and P. Mukherjee, Phys. Rev. D **74**, 083512 (2006) [arXiv:astro-ph/0607275].
- [43] http://lambda.gsfc.nasa.gov/product/map/current/likelihood_get.cfm
- [44] M. Kawasaki, K. Kohri and T. Moroi, Phys. Rev. D **71** (2005) 083502 [arXiv:astro-ph/0408426].

- [45] M. Kawasaki, K. Kohri and T. Moroi, Phys. Lett. B **625**, 7 (2005) [arXiv:astro-ph/0402490].
- [46] M. Kawasaki, K. Kohri and N. Sugiyama, Phys. Rev. Lett. **82**, 4168 (1999) [arXiv:astro-ph/9811437].
- [47] M. Kawasaki, K. Kohri and N. Sugiyama, Phys. Rev. D **62**, 023506 (2000) [arXiv:astro-ph/0002127].
- [48] S. Hannestad, Phys. Rev. D **70**, 043506 (2004) [arXiv:astro-ph/0403291].
- [49] K. Ichikawa, M. Kawasaki and F. Takahashi, Phys. Rev. D **72**, 043522 (2005) [arXiv:astro-ph/0505395].
- [50] K. Ichikawa, M. Kawasaki and F. Takahashi, JCAP **0705**, 007 (2007) [arXiv:astro-ph/0611784].
- [51] K. Kumekawa, T. Moroi and T. Yanagida, Prog. Theor. Phys. **92**, 437 (1994) [arXiv:hep-ph/9405337].
- [52] K. I. Izawa and T. Yanagida, Phys. Lett. B **393**, 331 (1997) [arXiv:hep-ph/9608359].
- [53] A. D. Linde, Phys. Lett. B **259**, 38 (1991).
- [54] A. D. Linde, Phys. Rev. D **49**, 748 (1994) [arXiv:astro-ph/9307002].
- [55] E. J. Copeland, A. R. Liddle, D. H. Lyth, E. D. Stewart and D. Wands, Phys. Rev. D **49**, 6410 (1994) [arXiv:astro-ph/9401011].
- [56] G. R. Dvali, Q. Shafi and R. K. Schaefer, Phys. Rev. Lett. **73**, 1886 (1994) [arXiv:hep-ph/9406319].
- [57] G. Lazarides, R. K. Schaefer and Q. Shafi, Phys. Rev. D **56**, 1324 (1997) [arXiv:hep-ph/9608256].
- [58] G. Lazarides and C. Pallis, Phys. Lett. B **651**, 216 (2007) [arXiv:hep-ph/0702260].
- [59] T. Moroi and T. Takahashi, Phys. Rev. D **66**, 063501 (2002) [arXiv:hep-ph/0206026].
- [60] D. H. Lyth, C. Ungarelli and D. Wands, Phys. Rev. D **67**, 023503 (2003) [arXiv:astro-ph/0208055].
- [61] D. H. Lyth and D. Wands, Phys. Rev. D **68**, 103516 (2003) [arXiv:astro-ph/0306500].
- [62] M. Zaldarriaga, Phys. Rev. D **69**, 043508 (2004) [arXiv:astro-ph/0306006].
- [63] N. Bartolo, S. Matarrese and A. Riotto, JCAP **0401**, 003 (2004) [arXiv:astro-ph/0309692].

- [64] F. Vernizzi, Phys. Rev. D **69**, 083526 (2004) [arXiv:astro-ph/0311167].
- [65] A. Jokinen and A. Mazumdar, JCAP **0604**, 003 (2006) [arXiv:astro-ph/0512368].
- [66] N. Barnaby and J. M. Cline, Phys. Rev. D **75**, 086004 (2007) [arXiv:astro-ph/0611750].
- [67] A. Chambers and A. Rajantie, Phys. Rev. Lett. **100**, 041302 (2008) [arXiv:0710.4133 [astro-ph]].
- [68] K. Ichikawa, T. Suyama, T. Takahashi and M. Yamaguchi, arXiv:0807.3988 [astro-ph].